OVEREXPRESSION OF SEQUESTOSOME-1 AS A PROTECTIVE MEASURE AGAINST OXIDATIVE STRESS IN THE RETINAL PIGMENT EPITHELIUM

By

DANIELLE LORNA LIVERPOOL

A THESIS PRESENTED TO THE GRADUATE SCHOOL
OF THE UNIVERSITY OF FLORIDA IN PARTIAL FULFILLMENT
OF THE REQUIREMENTS FOR THE DEGREE OF
MASTER OF SCIENCE

UNIVERSITY OF FLORIDA

2013

To the Great I Am

ACKNOWLEDGMENTS

I would like to acknowledge the following people who have been essential to the development of this thesis. Foremost, I would like to thank Dr. Alfred Lewin for his phenomenal support and guidance throughout this process. He has been a remarkable example of a mentor and an amazing scientist. I am tremendously grateful for his patience, insight, and encouragement throughout the past two years. I truly could not have asked for a better principal investigator. I thank my other committee members, Dr. Michael Boulton and Dr. William Hauswirth for their time, patience, and leadership. I thank the members of Dr. Lewin's and Dr. Boulton's laboratories for the knowledge that they have imparted to me and for their wonderful support and friendship. From these groups, I would specifically like to mention Dr. Haoyu Mao, Dr. CJ Song, Sayak Mitter, Brian Rossmiller, Hong Li, Dr. Manas Biswal, James Thomas, Jr., and Dr. Zhao-yang Wang for their recommendations and benevolence. I especially want to thank Dr. Cristhian Ildefonso for his unceasing assistance and encouragement during the execution of my project.

I thank my prior mentors for inspiring me to pursue this degree and allowing me to learn more about academia and about myself as a researcher: Dr. Mary Kay Schneider Carodine, Dr. Peter Kima, and Dr. Omar Oyarzabal. Finally, I would like to show my deepest gratitude to my family and friends, for they have been a source of strength and joy during my tenure as a graduate student.

TABLE OF CONTENTS

LIST OF TABLES

Table page

LIST OF FIGURES

LIST OF ABBREVIATIONS

4-HNE	4-Hydroxynonenal
AD	Alzheimer's Disease
AMD	Age-Related Macular Degeneration
AMP	Ampicillin
ARE	Antioxidant Response Element
ATCC	American Type Culture Collection
ATP	Adenosine Triphosphate
BSA	Bovine Serum Albumin
CBA	Chicken Beta-Actin
cDNA	Complementary DNA
CEP	Carboxyethylpyrrole
CMV-IE	Cytomegalovirus Immediate-Early
cPPT	Central Polypurine Tract
DMEM	Dulbecco's Modified Eagle's Serum
DMSO	Dimethyl Sulfoxide
ER	Endoplasmic Reticulum
FDA	Food and Drug Ddministration
FBS	Fetal Bovine Serum
GCL	Ganglion Cell Layer
GFP	Green Fluorescent Protein
GSTM1	Glutathione S-Transferase Mu 1
HEK	Human Embryonic Kidney
HO-1	Heme Oxygenase-1
INL	Inner Nuclear Layer

KEAP1	Kelch-like ECH Associated Protein 1
KIR	Keap1 Interacting Region
LDH	Lactate Dehydrogenase
LV	Lentivirus
MDA	Malondialdehyde
mtDNA	Mitochondrial Deoxyribonucleic Acid
MTT	3-(4,5-Dimethylthiazol-2-yl)-2,5-Diphenyltetrazolium Bromide
NAD(P)H	Nicotinamide Adenine Dinucleotide Phosphate
NQO1	NAD(P)H Quinone Oxidoreductase
NRF-2	Nuclear Factor Erythroid 2 Related Factor 2
ONL	Outer Nuclear Layer
OPL	Outer Plexiform Layer
PBS	Phosphate Buffered Saline Solution
POS	Photoreceptor Outer Segments
PuroR	Puromycin Resistance
ROS	Reactive Oxygen Species
RNS	Reactive Nitrogen Species
RRE	Rev Responsive Element
RPE	Retinal Pigment Epithelium
RT-PCR	Real-Time PCR
SQSTM1	Sequestosome-1
SV-40	Simian Virus 40
TNFα	Tumor Necrosis Factor Alpha
TRIS	Tris-Hydroxyethylaminomethane
VEGF	Vascular Endothelial Growth Factor

Abstract of Thesis Presented to the Graduate School
of the University of Florida in Partial Fulfillment of the
Requirements for the Degree of Master of Science

OVEREXPRESSION OF SEQUESTOSOME-1 AS A PROTECTIVE MEASURE AGAINST OXIDATIVE STRESS IN THE RETINAL PIGMENT EPITHELIUM

By

Danielle Lorna Liverpool

August 2013

Chair: Alfred S. Lewin
Major: Medical Sciences—Translational Biotechnology

Dry age-related macular degeneration is a multifactorial disease of the retina that can lead to the severe impairment of or complete loss of vision. Due to the variety of etiological factors involved, this disease has been difficult to treat. It is currently understood that accumulation of damage caused by excess oxidative stress in the eye contributes to pathogenesis of this disease. Our aim in this study is to prevent oxidative stress mediated damage in retinal pigment epithelial cells by increasing the transcription of antioxidant enzymes controlled by the DNA sequence called the Antioxidant Response Element (ARE). We attempt to stimulate this response by increasing the abundance of Sequestosome-1 (SQSTM1), a protein known to mediate the regulation of Nrf2, a transcription factor for several cytoprotective enzymes. We transfected ARPE-19 cells, a cell line of established human retinal pigment epithelial cells, with a plasmid expressing SQSTM1. Overexpression of this protein was verified by immunoblot analysis. Cells were exposed to either hydrogen peroxide or 4-hydroxynonenal to induce oxidative stress. LDH release assay and MTT assays were performed to characterize cytotoxicity and mitochondrial dehydrogenase activity, respectively. mRNA

levels of antioxidant enzymes were quantified by RT-PCR methods. Surprisingly, we discovered that increasing SQSTM1 abundance in ARPE-19 cells did not result in significant protection of cell viability as measured by the MTT assay or an increase in cytoprotective enzyme production. However, cytotoxicity was reduced in SQSTM1-expressing cells. SQSTM1 has several functions in addition to stimulation of the antioxidant response, including stimulation of autophagy. To further understand the mechanism of cytoprotection by gene delivery of *SQSTM1*, a stable cell line of ARPE-19 cells that displays constitutive expression of SQSTM1 was established.

CHAPTER 1
INTRODUCTION

The Mammalian Retina

The eye is composed of multiple types of tissue each with its own function, impact, and anatomical characteristics. The human eye is a conscious sense organ that permits the interpretation of motion, shape, contrast, color, and dimensions of objects by perceiving different wavelengths of light. This perception of light is required to initiate phototransduction. Phototransduction is the process by which photoreceptors absorb photons of light and transduce this information into an electrical response that can be relayed to the neural layers of the retina and ultimately, to the brain (Arshavsky, 2012). Diseases of the eye can result in skewed or decreased vision or even blindness, and therefore can be exceptionally detrimental to one's quality of life. The goal of this thesis is to describe the efforts to prevent the exacerbation of symptoms of a very common eye disease, dry age-related macular degeneration (dry AMD).

Anatomy of the Retina

A depiction of the structural organization of the retina can be found in Figure 1-1. The retina, composed of two delicate layers of tissue, is the innermost layer of the three layers of tissue that line the wall of the eyeball. From anterior to posterior, these three layers of tissue are the retina, the vascular choroid, and the sclera. The neural retina and the retinal pigment epithelium (RPE) are the two layers that form the retina (Khandhadia, 2012).

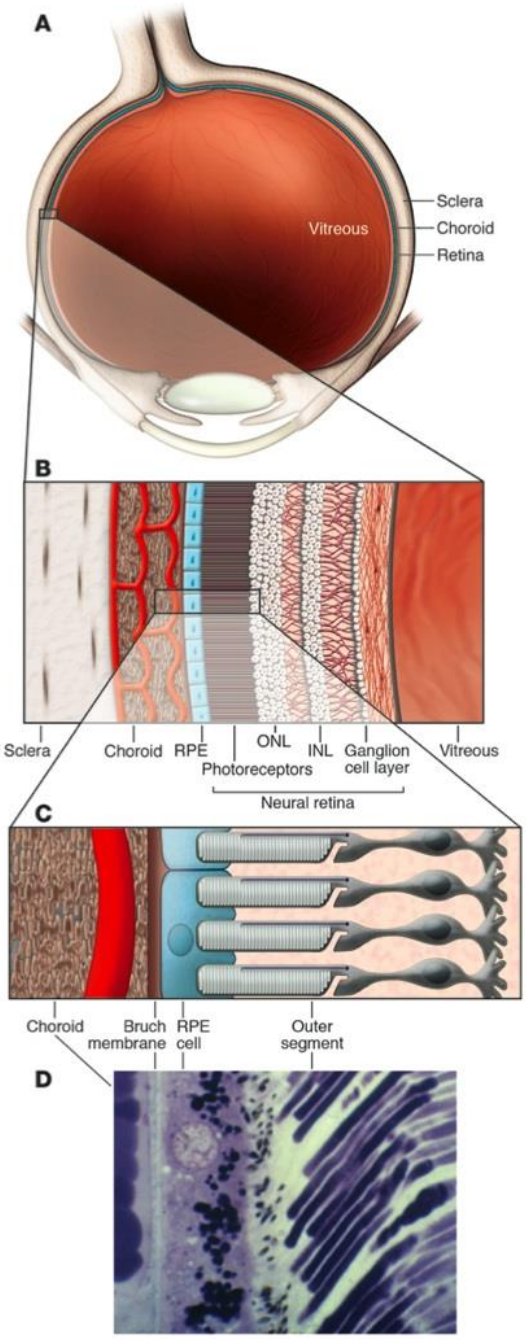

Figure 1-1. Anatomy of the Retina. A) A cross-section of the eye globe. B) A cross-section of the retina. The neural retina, which consists of the ONL, INL, GCL, and photoreceptors are located anterior to the RPE. C) Organization of the tissues in the posterior of the eyecup. D) A light microscopic view of the layers of the retina displayed in (C). This figure is adapted from reference (Bird, 2010).

The process of visual interpretation starts at the photoreceptors, where photons of light are absorbed by visual pigment and converted into an electrical signal that is relayed to bipolar cells in the outer plexiform layer (OPL) (Kaneda, 2013). The process by which absorbed photons are converted into electrical signals is known as phototransduction. In vertebrates, this mechanism transpires in the photoreceptor outer segment. Briefly, photons of light instigate the isomerization and activated form of rhodopsin, which activates the G protein transducin. Transducin activates an enzyme that hydrolyzes cGMP, which closes cGMP-gated channels and leads to hyperpolarization of the cell (Yau, 2009). The resulting electrical signal is processed and transmitted to retinal ganglion cells in the ganglion cell layer (GCL). During this step, visual information such as the color, contrast, brightness, and movement are perceived by amacrine cells and transferred to the optic nerve to be processed by the brain. Other cells in the retina such as amacrine cells and horizontal cells support signal modulation (Kaneda, 2013).

Retinal Pigment Epithelium

The RPE is a single monolayer of cuboidal pigmented epithelial cells that attach to each other via tight junctions. The RPE serves multiple functions in order to regulate retinal homeostasis (Barnett, 2012). Although separated from the choroid by Bruch's membrane, it transports ions, water, and metabolic end products from the subretinal space to the blood. It extracts nutrients such as glucose, retinol, and fatty acids from the blood and delivers them to photoreceptors. These cells also secrete growth factors that support the structural integrity of the photoreceptors and the surrounding retina. The RPE is in constant communication with photoreceptors, as it re-isomerizes molecules

necessary for the visual cycle and transports it to and from the photoreceptors. The outer segments of photoreceptors are structured as a stack of discs that contain pigments necessary for the visual cycle to occur. These discs are shed at the distal end of the segment, primarily with the first light of the morning and, importantly, phagocytosed by the RPE (Strauss, 2005). Undegraded material from this process can accumulate within RPE cells with age (Bird, 2010). Likewise, deficits in the RPE's quality control mechanisms can lead to the accumulation of lipofuscin granules that increases with aging (Rodríguez-Muela, 2013; Krohne, 2010). Failure of the RPE to perform its innate functions lead to deterioration of other cells in the retina (Bird, 2010).

Age- Related Macular Degeneration

Compromised function of the eye is a common trait in aging populations. A plethora of ocular diseases such as glaucoma, diabetic retinopathy, and age-related macular degeneration threaten the eyesight of the elderly population. Glaucoma, a degenerative optic neuropathy, is strongly correlated with increased intraocular pressure (Tezel, 2011). In the case of diabetic retinopathy, the structure and function of the retinal vasculature is compromised by persistent high glucose levels (Santos, 2012). Age-related macular degeneration (AMD) is a disease of the retina that leads to the distortion or loss of central vision. AMD is currently the leading cause of irreversible vision loss in the elderly in industrialized countries (Voleti, 2013).

Epidemiology

There are two related forms of AMD: exudative and non-exudative or atrophic. Exudative AMD, also referred to as "wet" AMD is characterized by the formation of new blood vessels that invade the space below the retina or the retina itself. This formation of blood vessels, termed choroidal neovascularization, can disrupt the structural

integrity of the retina, choroid, and Bruch's membrane (Voleti, 2013). The majority of the patients diagnosed with AMD have nonexudative, or "dry" AMD, a disease that lacks many of the complications associated with choroidal neovascularization. There are currently 8 million people in the United States (Klein, 2011) and more than 50 million people worldwide that are afflicted with age-related macular degeneration (Barnett, 2012). It is expected that approximately two-thirds of the population over the age of 80 will have some signs of AMD (Khandadia, 2012). Although the majority of the diagnoses are patients with dry AMD, 90% of severe vision loss can be attributed to patients with wet AMD. In wet AMD, blood vessels can grow from beneath the retina toward the macula. The combination of inflammation, angiogenesis, and tissue invasion within the eye globe lead to rapid onset of disease and loss of vision in wet AMD patients (Campa, 2010).

Both environmental and genetic factors contribute to the pathogenesis of this disease. Age and smoking are two of the highest risk factors for AMD. The cell types most affected include photoreceptors, the RPE, Bruch's membrane, and the choroid. Genetic studies have concluded that misregulation of the immune system can serve as a contributing factor in AMD (Barnett, 2012).

Role of Oxidative Stress in AMD

Reactive oxygen species (ROS) and reactive nitrogen species (RNS) are involved in several processes that are vital for proper cellular function. Cellular function can be disrupted in the event that there is a surplus or deficit of ROS in the cell. Oxidative stress is the state in which the amount of ROS present in the cell is greater than what the cell can efficiently detoxify (Halliwell, 2006). ROS are relatively short-lived within the cellular environment but damage caused by these species can

accumulate. All ROS in the cell are not eliminated because ROS perform important functions. In the event that the amount of ROS is greater than what the cell is equipped to keep at bay, the cell will mount defenses such as antioxidants to eliminate these species and minimize damage (Halliwell, 2006). Enzymes such as superoxide dismutases and catalases in addition to other antioxidant and cytoprotective factors demonstrate the ability to reduce or neutralize ROS levels in the cell. Glutathione (GSH) neutralizes lipid peroxides and H_2O_2. Melanin is a pigment molecule that offers protection. Vitamins such as α-tocopherol and ı-ascorbate also contribute to the maintenance of cellular redox homeostasis (Plafker, 2012).

Oxidative stress can originate from either exogenous or endogenous sources. Exogenous stressors, such as cigarette smoke, can instigate the production of chemical oxidants that will modify existing proteins, DNA, and lipids in the retina (Barnett, 2012). These oxidation events result in the formation of reactive molecules and advanced glycation end products that can cause damage to the sensitive tissue. Some of the molecules that have been found as a result of these incidences are 4-hydroxynonenal (4-HNE), malondialdehyde (MDA), and carboxyethylpyrrole (CEP). Proper regulation of the environmental balance of the retina is achieved by crosstalk between various elements of the eye. The retina has the richest oxygen demand by weight of any organ in the body. The RPE is situated in a location in the eye that makes it very susceptible to oxidative stress (Barnett, 2012).

Role of Mitochondrial Function in AMD

The mitochondrion is an organelle necessary for proper cellular function and survival by serving as a key regulator of the cell's metabolic activities. In mammals, oxidative phosphorylation is the process by which mitochondria oxidize nutrients to form

adenosine triphosphate (ATP), a molecule that supplies energy for metabolic events. Mitochondria function in fatty acid oxidation, amino acid and heme biosynthesis, antioxidant regulation, apoptosis, and cytoprotection (Olszewska, 2013).

Mitochondrial decay is a normal result of cellular aging. Increased chronological age results in increased damage to mtDNA, reduced activity of the enzymes that perform in the respiratory chain, ROS imbalance, and decreased ability to defend against oxidative stress (Wenzel, 2008). There is growing evidence that confirms that mitochondrial impairment and the absence of effective mtDNA repair can contribute to pathogenesis in degenerative retinal diseases and diseases related to aging (Jarrett, 2010). Mutations in mitochondrial DNA may lead to severe congenital defects affecting the endocrine system the central nervous system, the heart and the musculoskeletal system (Koopman, 2007). More commonly, however, mitochondrial defects have been associated with neurodegenerative diseases such as Parkinson's disease and Alzheimer's disease (AD). Specifically, in AD, dysfunction of the ETC, increased oxidative stress, subcellular fractionation, misregulation of Ca^{2+} content, mtDNA mutations, and an impaired balance of fusion and fission are some of the factors that contribute to pathogenesis. Redistribution of mitochondria is also noted in the AD-afflicted hippocampus and neurons (DuBoff, 2013).

The uniformity and integrity of the mitochondria shape, size and function correlates with the cell's metabolic activity and state of replication. Alterations in lipid peroxidation, cytoplasmid superoxide dismutases, and oxidative stress markers have been observed in aging cells (He, 2010). Importantly, cellular ROS content can serve as a determinant of mitochondrial shape and function (Koopman, 2007).

Cellular stress may serve as the impetus for changes in mitochondrial functions. Endoplasmic reticulum (ER) stress leads to misregulation of respiratory activities and activates apoptotic pathways in the mitochondria (Kwong, 2007). Excess oxidative stress inhibits proper regulation of oxidative phosphorylation and causes mitochondrial fragmentation (Koopman, 2007). Due to the close proximity of mitochondrial DNA (mtDNA) to the oxygen-radical producing respiratory chain, mtDNA is more vulnerable to oxidative damage than nuclear DNA (Olszewska, 2012).

In the event that the homeostatic state of mitochondria is disrupted, ATP synthesis is disturbed, which can lead to the production of excess ROS and proteins that participate in cell death pathways, such as apoptosis, autophagy, or mitotic catastrophe (Blasiak, 2013). Cells are enabled with a defense mechanism that sequesters and degrades dysfunctional mitochondria before it causes cell death. The process by which mitochondria are selectively sequestered and targeted for destruction is known as mitophagy. It is possible for mitochondria to activate both cell death and mitophagy, two different processes, in response to the same stimulus. (Kubli, 2012). Overall, the state of mitochondrial health can greatly affect overall cellular viability.

Nuclear factor-erythroid 2 related factor 2

Normal aerobic metabolic activity results in the production of ROS in unstressed conditions. In order to control the redox status of the cell and to eliminate ROS that are not needed for proper cellular function, a *cis*-acting element termed the Antioxidant Response Element (ARE) is transcribed to produce cytoprotective enzymes that detect and eliminate excess ROS (Nguyen, 2009). The ARE is found in the 5’ flanking region of phase II detoxification enzymes (Liu, 2007). The ARE is activated in response to reactive oxygen species and other electrophilic compounds that have the ability to

undergo redox cycling (Nguyen, 2009), a series of chemical reactions that result in the production of the reactive species (Gutierrez, 2000). The prominence of the ARE in maintaining endogenous redox has been demonstrated in several studies that conclude that *nrf2*$^{-/-}$ mice lack the ability to mount a response to oxidative stress via ARE-controlled genes (Nguyen, 2009). Glutathione S-transferases (GST), heme-oxygenase 1 (HO-1), and NAD(P)H: quinone oxidoreductase 1 (NQO1) are some genes that are activated by the ARE (Liu, 2007).

The transcription factor nuclear factor-erythroid 2 related factor 2 (Nrf2) is a leucine zipper transcription factor that regulates the expression of a number of genes that are transcribed in response to electrophiles, pro-oxidants, ROS, or RNS. Nrf2 is regulated in part by the cytosolic metalloprotein Kelch-Like ECH-associated protein 1 (Keap1). This interaction is depicted in Figure 1-2. The Neh2 domain of Nrf2 interacts with the Kelch repeat domain of Keap1. This interaction is disrupted in response to reactive species in the cell. This occurrence is the impetus for Nrf2 translocation to the nucleus, where it binds to the ARE and promotes transcription of the antioxidant regulators mentioned previously. The activation of the Nrf2 antioxidant and cellular detoxification program is one of the cell's most powerful defenses against oxidative stress (Tew, 2011).

Sequestosome-1/p62

Sequestosome-1 (SQSTM1), or p62, is a 65 kDa protein located in both the cytoplasm and the nucleus in order to participate in protein trafficking and ubiquitination events. SQSTM1 participates in the mediation of several signaling pathways. In addition to its role in the nucleus as a transcriptional co-activator, SQSTM1 serves as a modifier of the K^+ channel, scaffold in TNFα and IL-8 pathways, and a molecular bridge in the

process of selectively activating NF-κB. The UBA domain in the C-terminus of SQSTM1 has an affinity for polyubiquitinated proteins and serves to recruit and bind ubiquitinated proteins (Fig. 1-2) (Geetha, 2002).

Importantly, SQSTM1's KEAP1 interacting region (KIR) motif binds to the Kelch repeat domain of KEAP1, the location of Nrf2/Keap1 binding. SQSTM1 serves as a competitor of Nrf2 binding, which promotes free cytosolic Nrf2 (Nezis, 2012). In addition to having multiple binding partners that participate in different cellular pathways, SQSTM1 has the unique ability to homodimerize and polymerize itself. This conformation, however, does not prevent the binding of SQSTM1 to Nrf2 or KEAP1 (Nezis, 2012). Interestingly, SQSTM1 has an ARE DNA element in its promoter, permitting positive induction of SQSTM1 transcription via Nrf2. Therefore, Nrf2 and SQSTM1 are in a positive feedback loop, where Nrf2 increases SQSTM1 production and SQSTM1 encourages nuclear translocation of Nrf2 (Jain, 2010).

SQSTM1 plays a crucial role as a cargo receptor in the regulation of autophagy. Autophagy is a process that is obligatory for cell survival, maintenance, and differentiation. This process involves the collection of cytosolic contents into a double-membrane vacuole to form an autophagosome. The autophagosome then fuses with and releases its contents into lysosomes, where acid hydrolases degrade the cellular material (Fan, 2010). In the event that proteins for potentially harmful aggregates or are misfolded, ubiquitin molecules are added to the structures to target them for degradation. SQTSM1 recognizes mono- and polyubiquitinated structures via its UBA domain and assists in delivery of the targeted assemblies to autophagic machinery. Inhibition of autophagy results in the accumulation of ubiquitinated protein aggregates,

which can be a source of cellular toxicity (Schreiber, 2013). Through polymerization of its PB1 domain, SQSTM1 is recruited to mitochondrial substrates by the E3 ubiquitin ligase Parkin, which ubiquitinates specific protein substrates on damaged mitochondria. SQSTM1 then serves to mediate aggregation of ubiquitinated mitochondria for targeted destruction, similar to its role in the aggregation of ubiquitinated proteins. (Narendra, 2010). Recruitment of SQSTM1 alone is not sufficient for induction of mitophagy, but it has been reported that knockdown of SQSTM1 substantially inhibits mitophagy (Kubli, 2012).

SQSTM1 (here also referred to as p62) forms protein bodies, or p62 bodies, that consist of accumulations of SQSTM1 and ubiquitinated proteins. p62 bodies either reside in the cytosol, nucleus, or are present within autophagosomes and lysosomal structures. In order for formation of p62 bodies, the UBA domain of SQSTM1 must be present and unbound to other proteins (Bjørkøy, 2005). The PB1 domain of SQSTM1 is necessary for SQSTM1 to interact with itself. These protein bodies are found both as membrane-free protein aggregates (sequestosomes) and as membrane-confined autophagosomal and lysosomal structures (Bjørkøy, 2005).

SQSTM1, as a protein, is involved in numerous pathways that arbitrate regulation of cellular function. Although it is primarily regarded as a cytosolic protein, it contains both a nuclear localization signal (NLS) and nuclear export signal to facilitate transport between the two compartments (Pankiv, 2010). The interplay between the various pathways in both homeostatic and perturbed conditions is of great interest in relation to RPE function in AMD.

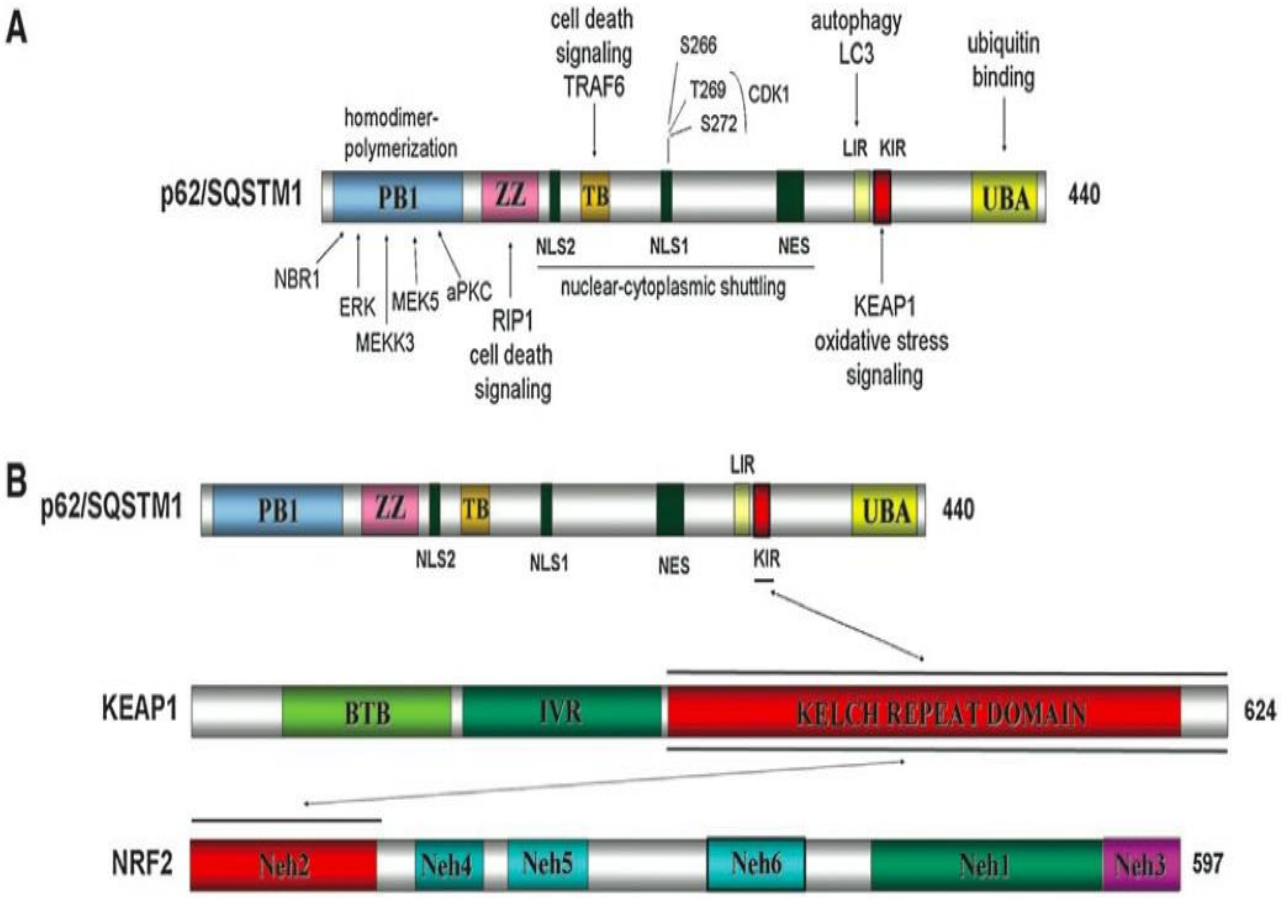

Figure 1-2. An illustration of the structure, function, and binding interactions of Sequestosome-1 (SQSTM1/p62). A) Sequestosome-1 acts as a scaffolding protein that serves in many pathways. The different domains of SQSTM1 are responsible for mediating its activity in different pathways associated with cell survival, protein trafficking, and proliferation. B) The Keap-1 Interacting region (KIR) in the C-terminus of SQSTM1 binds to the Kelch repeat domain of KEAP1. This same domain regulates abundance of cytosolic Nrf2 by binding to its Neh2 domain in the N-terminus. This figure was adapted from reference (Nezis, 2012).

Treatments for AMD

Although treatments approved by the U.S. Food and Drug Administration (FDA) have been identified and are currently being utilized for exudative AMD, no FDA-

approved treatments or preventative measures for non-exudative AMD exist (Voleti, 2013). Vascular endothelial growth factor (VEGF) is a circulating serum cytokine that promotes angiogenesis and vascular permeability. Inhibition of VEGF activity has been the foremost method for treatment of choroidal neovascularization. This is being achieved through use of antibody fragments that bind to all VEGF isoforms (Ranibizumab), RNA aptamers that inhibit VEGF from binding to its receptor (Pegaptanib), and receptor decoys that trap VEGF (Aflibercept) (Cheung, 2013). A more thorough understanding of the pathogenesis of the disease is needed before effective therapeutic treatments can be developed.

Specific Background and Objectives: After exposure to oxidative or electrophilic species, one or more of KEAP1's cysteine residues undergo oxidation, leading to a conformational change in the protein. This change inhibits KEAP1 from serving as a substrate ubiquitin ligase adaptor, therefore discontinuing the targeted destruction of Nrf2. This sequence of events leads to the increased translocation of Nrf2 from the cytosol to the nucleus, where it can then increase transcription of ARE enzymes (Jain, 2010).

Several studies have demonstrated that the activation of the ARE by manipulation of the Nrf2/Keap1 pathway have facilitated *in vitro* protection from oxidative stress (Reuland, 2012; Ha, 2006). A 48-hour transfection of SQSTM1 encoding cDNA into primary cortical neurons doubled the amount of nuclear Nrf2 protein levels and increased ARE cDNA levels (Liu, 2007). With the results of these experiments in mind, the goal of this project is to determine if overexpression of SQSTM1 can protect retinal pigment epithelial cells from oxidative stress. To

accomplish this, I proposed the following aims: I) To achieve increased expression of *SQSTM1* in ARPE-19 cells using transfection-based methods. II) To determine the impact of varying concentrations of hydrogen peroxide or 4-hydroxynonenal on cell survival. III) To assess the ability of SQSTM1 to mediate protection of ARPE-19 cells exposed to oxidative stress. IV) To measure the effect of SQSTM1 overexpression on regulation of ARE antioxidant enzymes.

CHAPTER 2
MATERIALS AND METHODS

DNA Techniques

Preparation of Plasmid DNA

The pTR-SB-smCBA-SQSTM1 plasmid DNA (Fig. 2-1) was a gift from Dr. Diego Fajardo. The pTR-smCBA-hGFP plasmid DNA (Fig. 2-1) was graciously supplied by Dr. Cristhian Ildefonso. Both plasmids contain a cytomegalovirus immediate-early enhancer (CMV-IE) coupled to a strong and constitutively active chicken-beta actin promoter to maximize gene expression. The ampicillin resistance gene (AmpR) was used as a marker for selective propagation of bacteria. The vector includes a chimeric intron to increase transgene expression and a bacteriophage f1(+) origin of replication. To ensure fidelity of the plasmid DNA, sequencing of the DNA was executed by the DNA Sequencing Core Facility, Interdisciplinary Center for Biotechnology Research (ICBR) at the University of Florida.

Transformation

E. coli SURE (Invitrogen) cells were used for the transformation of the plasmids used in downstream experiments. Electroporation was performed at 1.5 volts for 5 msec in chilled 1mm plastic cuvettes. Cells were allowed to recover in 500 µL SOC medium (Life Technologies) by incubating at 37 °C for 1 hour in a shaking incubator. Recovered cultures were spread on Luria Bertani Broth (LB) agar plates containing 100 µg/mL ampicillin (amp) to select for transformed cells. Plates were incubated overnight (12 – 16 hours) at 30 °C.

Plasmid Maxi-Preparation

Colonies containing a single clone were selected after the overnight incubation. Individual clones were chosen from the agar plates and 50 mL flasks containing 5 mL LB and ampicillin were inoculated with a single colony of transformed bacteria. Samples were incubated in a shaking water bath at 37 °C for approximately 8 hours. The samples were then added to 145 mL LB containing 100 µg/mL ampicillin and incubated 37 °C overnight in a shaking water bath. Plasmid DNA was isolated using the Plasmid Maxi Kit (Omega Bio-Tek). Purified plasmid DNA was eluted in sterile, double-distilled water and stored at -20°C.

A

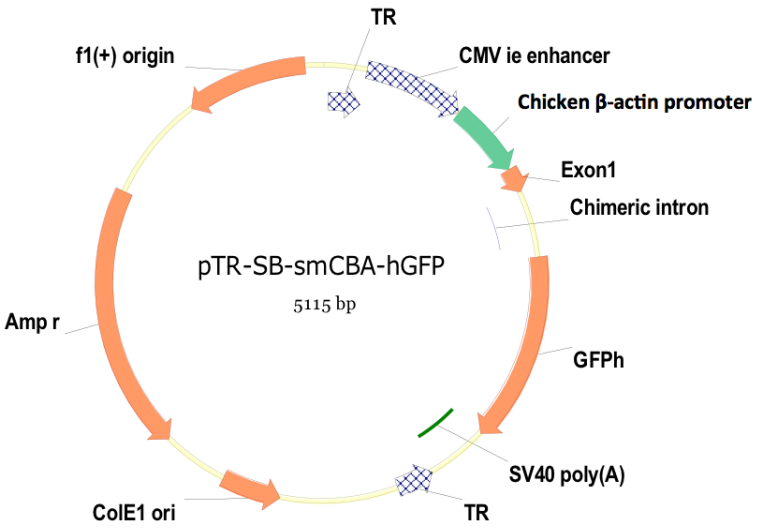

B

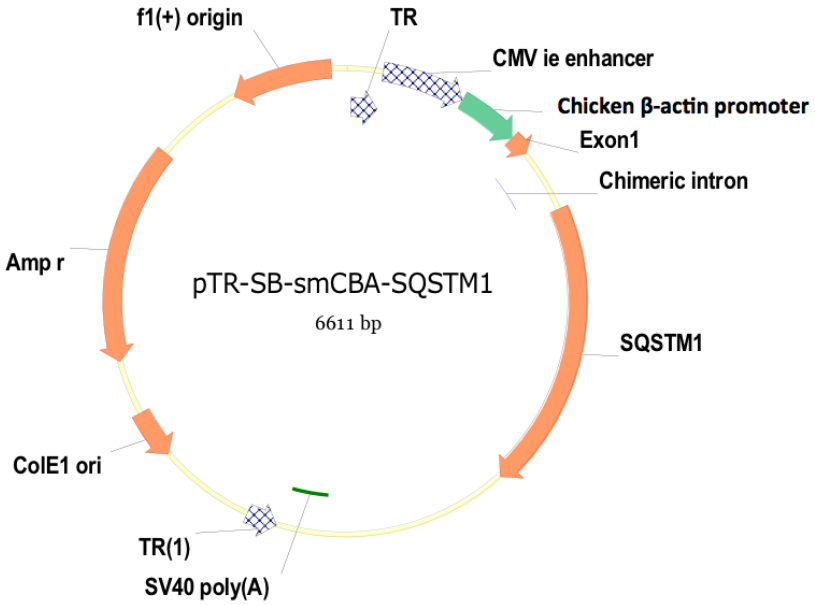

Figure 2-1. Plasmids used for transfection of ARPE-19 cells. A) Plasmid map of pTR-SB-smCBA-SQSMT1. B) Plasmid map of control vector pTR-SB-smCBA-hGFP. Plasmids were introduced into ARPE-19 cells using NovaFector transfection reagent (Venn Nova). The Cytomegalovirus immediate-early (CMV-IE) enhancer and the chicken beta-actin promoter were included to increase gene expression. TR: terminal repeat, SV40: Simian virus 40 poly (A) tail; AmpR: Ampicillin resistance gene; SB: simple basic.

Tissue Culture Techniques

This section describes the general maintenance and specific techniques employed while using an established human cell line of retinal pigment epithelial cells. The cell line, ARPE-19, is a spontaneously arising human RPE cell line with normal karyology that forms a polarized monolayer *in vitro* (Dunn, 1996).

Cell Culture

ARPE-19 cells were obtained from American Type Culture Collection (ATCC) at ampule passage number 19 and immediately reconstituted according to the supplier's protocol. Cells were cultured in Dulbecco's modified Eagle's serum: Nutrient Mixture F-12 (DMEM/F-12), supplemented with 10% fetal bovine serum (GIBCO) (FBS), 100 U/mL penicillin, 100 µg/mL streptomycin, and 2 mM L-glutamine. This mixture will be referred to as "complete medium". Cells were incubated at 37 °C with 5% CO_2 until 85% confluence. All experiments were performed with cells between passages 21 and 41.

Transfections

ARPE-19 cells were counted by trypan blue exclusion using a hemacytometer. Depending on the assay that was going to be performed, cells were seeded in tissue-culture treated plates (Genesee Scientific) with the appropriate number of wells and incubated overnight for 12-16 hours in complete DMEM/F-12 to allow them to attach to the plate. After the overnight incubation, the plasmid DNA was diluted in Opti-MEM reduced serum medium (Invitrogen). NovaFECTOR (Venn Nova), the transfection reagent, was added to the plasmid DNA at 4 µg of reagent per µg of plasmid DNA. Solutions were prepared according to the number of cells that were seeded. Dilutions of the DNA were performed so as to deliver 0.5 µg, 1.5 µg, or 2.5 µg of DNA to the cells.

The DNA and reagent were incubated in Opti-MEM (Invitrogen) at room temperature for 30 minutes to allow the reagent to form a complex with the DNA. Cells were washed with phosphate buffered saline (PBS) (GIBCO) (1.06 mM KH_2PO_4, 155.17mM NaCl, 2.97 mM Na_2HPO_4-$7H_2O$) to remove any residual serum from the medium that may lower transfection efficiency. The cells were incubated with the DNA and transfection reagent mixture for 6 hours at 37 °C. The mixture was removed and the cells were incubated in DMEM/F-12 for an additional 42 hours to accomplish a 48-hour transfection.

Induction of Oxidative Stress

Hydrogen peroxide (Sigma) (H_2O_2) was used to induce oxidative stress to the cells. The solution was always prepared fresh by diluting stock H_2O_2 in Opti-MEM to final concentrations of 200 µM, 400 µM, 600 µM, or 800 µM. At the end of the 48-hour transfection, cells were washed once with PBS to remove lingering medium. Samples were incubated with the freshly prepared solution containing H_2O_2 for six hours at 37 °C with 5% CO_2. Stock H_2O_2 was stored at 4°C and in the dark to prevent decomposition of the solution.

In a similar manner, 4-Hydroxynonenal (Calbiochem) (4HNE) was diluted in PBS to final concentrations of 5 µM, 10 µM, 20 µM, 40 µM, or 60 µM. Solutions were prepared during the last hour of the 48-hour transfection and added to the cells immediately following the end of the transfection period. Samples were incubated with the diluted 4HNE solutions for six hours at 37 °C with 5% CO_2. Stock solutions of 4HNE were stored at -80°C to preserve chemical activity.

RNA Techniques

RNA Extraction

RNA was extracted from samples after transfection and induction of oxidative stress using the RNeasy RNA extraction kit (Qiagen) according to the manufacturer's protocol. RNA was eluted in 50 µL sterile double-distilled water. Samples were quantified by spectrophotometry by reading the OD_{260}. The purity of the RNA was determined by analyzing the OD_{260}/OD_{280} ratio.

Real-Time PCR

Real-Time PCR (RT-PCR) was a technique used to quantify the production of mRNA for different antioxidant enzymes after stimulation of ARPE-19 cells by oxidative stressors. From the purified RNA, first-strand cDNA synthesis from 1 µg of RNA of each sample was executed using the iScript cDNA synthesis kit (Bio-Rad). Reactions were completed in a final volume of 20 µL. Briefly, each reaction was performed by mixing 5 µL SsoFast Evagreen mix (Bio-Rad), 2 µL water, 1 µL of 3 µM sense primer for one gene, 1 µL of 3 µM antisense primer for the same gene, and 1 µL of cDNA for one sample. Primer sequences are listed in Table 2-1. The total volume for each reaction was 10 µL. The reactions were loaded in a 96-well plate, sealed, and centrifuged at 7,600 x g for 2 minutes. The reaction mixture was then subjected to optimized reaction conditions listed in Table 2-2 using the CFX96 Touch RT-PCR Detection system (Bio-Rad). Gene expression was extrapolated from the data after analyzing with CFX Manager Software (Bio-Rad).

Table 2-1. Oligonucleotide primers used for mRNA level detection in RT-PCR

Primer	Orientation	Sequence
GAPDH	Sense	5'- GAG TCA ACG GAT TTG GTC GT -3'
GAPDH	Antisense	5'-TTG ATT TTG GAG GGA TCT CG -3'
GSTM1	Sense	5'- ATG CCC ATG ATA CTG GGG TA -3
GSTM1	Antisense	5'- GTG AGC CCC ATC AAT CAA GT -3'
HO-1	Sense	5'- ACA TCT ATG TGG CCC TGG AG -3'
HO-1	Antisense	5'- CGC TTC ACA TAG TGC TGC AT -3'
NQO1	Sense	5'- AAA GGA CCC TTC CGG AGT AA-3'
NQO1	Antisense	5' CCA TCC TTC CAG GAT TTG AA -3'

Table 2-2. RT-PCR conditions

Step	Temperature	Duration
1	95.0 °C	3:00
2	95.0 °C	0:10
3	60.0 °C	0:20
4	Go To Step 2 39 more times	N/A
5	95.0 °C	0:30
6	55.0 °C	0:30
7	Melt curve 60 °C to 95 °C increment 0.5 °C	0:50
8	4.0 °C	Indefinite
9	END	N/A

Protein Techniques

Protein Extraction from cells

ARPE-19 cells were rinsed with sterile PBS to remove any residual medium. The cells were trypsinized and collected in a 1.5 mL microcentrifuge tube. The cells were centrifuged at 16,00 x g for 1 minute at room temperature in an Eppendorf 5415C centrifuge. The trypsin was discarded. Pellets were washed once with PBS to remove remaining trypsin and centrifuged for 5 minutes at 16,000 x g at room temperature. The wash buffer was discarded. Pellets were stored at -80°C until they were ready to be utilized in later experiments.

Cell pellets were removed from -80°C, placed on ice, and resuspended in 200 µL RIPA buffer containing 1% Protease Inhibitor (Sigma Aldrich) and 1% 0.5 M EDTA. Samples were mixed by vortexing every 10 minutes for 30 minutes to complete cell

lysis. Samples were centrifuged at 1400 x g for 15 minutes at 4°C to pellet extracellular material. Supernatant was collected and transferred to a 1.5 mL microfuge tube. 120 µL of the supernatant was added to 30 µL freshly prepared Laemmli sample buffer (Laemmli, 1970) and heated at 97°C for 5 minutes to denature and dissociate proteins.

Protein Quantitation

Protein concentration was determined using a DC Protein Colorimetric Assay (Bio-Rad). Samples of cell supernatant were loaded in triplicate onto an optically clear 96-well plate. A standard curve using known concentrations of bovine serum albumin (BSA) (Promega) was generated to determine the sample protein concentration. The standard curve ranged from 0.30 mg/mL to 1.5 mg/mL of BSA diluted in RIPA buffer. Absorbance values were read at 750 nm after the required incubation period.

Protein Extraction and Immunoblot Analysis

Immunoblot analysis was performed using Tris-HCl ready gels containing 10% polyacrylamide (Bio-Rad). 20 µg of protein were loaded for each sample. The gel was run at approximately 250 Volts for 2 hours. Proteins were transferred to a 0.2 µm polyvinylidene fluoride membrane using an iBlot gel transfer device (Invitrogen). The protein transfer was performed for 7 minutes.

Blocking of Membrane and Application of Antibodies

Membranes were incubated in methanol for 5 minutes at room temperature prior to blocking. Membranes were then blocked in blocking buffer (Odyssey) for 30 minutes, shaking, at room temperature. Primary antibodies were diluted in fresh blocking buffer using the dilution scheme displayed in Table 2-3. Primary antibodies were applied overnight by incubating the membranes at 4°C, shaking, for 12-16 hours. Membranes were then washed with PBS + 0.1% Tween® 20 (Fisher Scientific) (PBS/Tween) three

times for 5 minutes. Secondary antibodies were diluted in PBS/Tween as described in Table 3-3. Membranes were incubated with infrared-labeled secondary antibodies for 1 hour, shaking, at room temperature. Imaging was performed using a quantitative fluorescence imaging system at the appropriate wavelengths. Images of the bands were digitized and densitometric analysis was performed using ImageJ.

Table 2-3. List of antibodies utilized for immunoblot analysis

Antibody	Vendor	Dilution
Mouse Anti-p62 Lck ligand	BD Biosciences	1:4000
Rabbit Anti-GFP	Invitrogen	1:5000
Rabbit Anti-β-Actin	Odyssey	1:5000
Goat Anti-Mouse	Odyssey	1:5000
Goat Anti-Rabbit	Odyssey	1:5000

Creation of Lentivirus-transduced Stable Cell Lines

Transformation

DH5-α (Invitrogen) cells were used for the transformation of bacteria with the plasmids shown in Fig. 3-3. Expression of SQSTM1 and GFP were under the control of the elongation factor 1-alpha (EF1) promoter. The HIV-1 long terminal repeat (LTR) served as part of the promoter but also allowed the lentivirus vector to integrate into the genome of both dividing and non-dividing cells (Moldt, 2011). A T2A reporter peptide gene was included to track cells that were actively expressing the gene of interest. The puromycin resistance gene allowed for selection of transduced cells that were expressing the gene of interest. The ampicillin resistance (AmpR) gene and pUC origin

of replication allow for selection and propagation in bacteria. DH5-α aliquots were incubated on ice with 2 µL plasmid DNA for 5 minutes. The bacterial cells were subjected to heat shock at 42°C for 1.5 minutes and immediately placed on ice for 2 minutes. The cells were allowed to recover in 500 µL SOC medium (Life Technologies) by incubating at 37 °C for 1 hour in a shaking incubator. Recovered cultures were spread on Luria Bertani Broth (LB) agar plates containing 100 µg/mL ampicillin (amp) to select for transformed cells. Plates were incubated overnight (12 – 16 hours) at 30 °C. 10 mL LB broth containing 100 µg/mL ampicillin were inoculated with one transformed colony and incubated overnight at 37 °C. Plasmid DNA extraction from bacterial cells was performed using the PureLink Quick Plasmid Miniprep Kit (Invitrogen) according to the manufacturer's protocol.

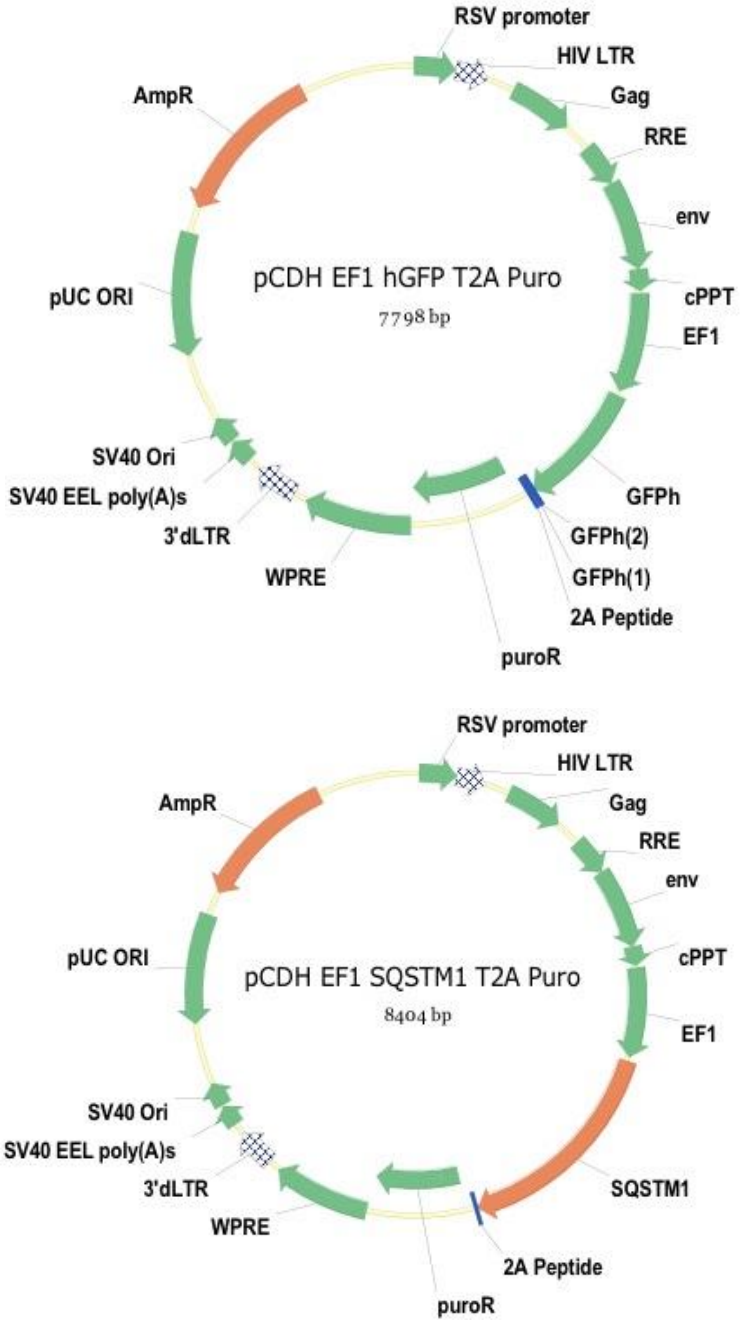

Figure 2-2. Plasmids used for lentiviral vector mediated delivery of SQSTM1 or GFP. The Puromycin resistance (PuroR) sequence allows for selection of ARPE-19 cells that have incorporated the plasmid of interest. RSV: Rous sarcoma virus promoter; LTR: long terminal repeat; RRE: rev responsive element; WPRE: woodchuck hepatitis posttranscriptional regulatory element; cPPT: central polypurine tract; EF1: elongation factor 1 alpha promoter.

Packaging of Virus

Human Embryonic Kidney 293T (HEK293T) cells were seeded at $3x10^6$ cells per well in 10 cm plates containing complete medium and incubated overnight at 37 °C with 5% CO_2. After the overnight incubation, the growth medium was replaced with 9 mL of transfection medium (DMEM/F-12 supplemented with 10% FBS). In a microcentrifuge tube, 2.0 µg of pCDH-EF1-hGFP-T2A-Puro plasmid DNA or pCDH-EF1-SQSTM1-T2A-Puro plasmid DNA was diluted in 400 µL of sterile Opti-Mem. Twenty microliters of pPACK-HI packaging plasmid mix (Systems Biosciences) was added to each mixture and incubated at room temperature for 15 minutes. In a separate microcentrifuge tube, 30 µL of Lipofectamine 2000 (Invitrogen) reagent was added to 370 µL of Opti-Mem. The diluted Lipofectamine solution was added dropwise to the diluted DNA mixture and mixed by gentle pipetting. The transfection mixture of Lipofectamine and DNA was incubated at room temperature for 15 minutes to allow the reagent to form a complex with the DNA. The complexed DNA was then added dropwise to the HEK293T cells. The HEK293T cells were incubated with the DNA/Lipofectamine complex at 37 °C with 5% CO_2 for 48 hours.

After the 48-hour transfection period, the cell supernatant was harvested and centrifuged at 1,811 x g at room temperature for 5 minutes to pellet cellular debris that still remained in the medium. The supernatant containing the viral particles was sterilized using a 0.2 µm nylon syringe filter (Fisher Scientific) and stored in 1 mL aliquots at -80°C.

Transduction

1 x 10^6 ARPE-19 cells were seeded in T-25 flasks in DMEM/F-12 (supplemented with 10% FBS, 100 U/mL penicillin, and 100 µg/mL streptomycin) and incubated

overnight to permit attachment to the flask. Five hundred microliters of viral supernatant was recovered from -80°C and added to the cells following the overnight incubation. The cells were incubated with the sterilized supernatant for 48 hours at 37 °C with 5% CO_2.

Selection

In order to ensure that cells expressed the plasmid of interest, cells were incubated with puromycin to exterminate cells that did not have the DNA incorporated into the cellular genome. Transduced ARPE-19 cells were rinsed with PBS. Cells were then incubated in complete medium supplemented with 1 µg/mL puromycin (Life Technologies) for 72 hours. Wild-type ARPE-19 cells of the same passage were included as a negative control. The negative control was incubated with this complete medium supplemented with puromycin to ensure destruction of all cells that did not contain the plasmid DNA.

Microscopy

Fluorescence microscopy was performed to characterize expression of GFP in the GFP stable cell line. A Keyence BZ-9000 inverted fluorescent microscope was used to obtain images of the cells. Images of live cells in complete medium were obtained using a 10X objective and analyzed using BZ-II Analyzer software (Keyence).

Immunoblot Analysis

While the stable cells were trypsinized during routine passaging, aliquots of 1 x 10^5 stable cells were collected in microcentrifuge tubes and pelleted by centrifugation at 7,200 x g for 2 minutes. Cell pellets were rinsed with PBS and centrifuged again at the same conditions. Cell pellets were resuspended in 200 µL RIPA buffer containing 1% Protease Inhibitor (Sigma Aldrich) and 1% 0.5 M EDTA. Samples

were vortexed every 10 minutes for 30 minutes to complete cell lysis. Samples were centrifuged at 1400 G for 15 minutes at 4°C to pellet extracellular material. Supernatant was collected and transferred to a 1.5 mL microfuge tube. 120 µL of the supernatant was added to 30 µL freshly prepared Laemmli sample buffer (Laemmli, 1970) and heated at 97°C for 5 minutes to denature and dissociate proteins. Protein concentration was determined using a DC Protein Colorimetric Assay (Bio-Rad).

Functional Assays

Thiazolyl Blue Tetrazolium Bromide (MTT) Assay

In order to determine cellular metabolic activity, a functional assay that utilizes (3-(4,5-Dimethylthiazol-2-yl)-2,5-diphenyltetrazolium bromide (MTT) (Sigma) was performed. MTT is a tetrazolium dye that is reduced to formazan by mitochondrial dehydrogenases. ARPE-19 cells were seeded at 30,000 cells/well in a 96-well tissue-culture treated plate (Olympus) and transfected according to the steps previously described. The cells were subjected to oxidative stress by adding either H_2O_2 or 4HNE diluted in the appropriate solvent for 6 hours. MTT powder was diluted in RPMI-1640 (Invitrogen) medium without phenol red to a final concentration of 5 mg/mL to create the stock solution. MTT stock solution was filter-sterilized using a 0.2 µm nylon syringe filter (Fisher Scientific) and added to RPMI-1640 to a final volume of one-tenth of the culture solution. Samples were incubated in 200 µL of diluted MTT solution for 3.5 hours. The MTT solution was carefully aspirated and formazan crystals were dissolved in 200 µL dimethyl sulfoxide (DMSO) (Fisher Scientific). Absorbances were read at 750 nm using a spectrophotometer.

LDH Release Assay

Plasma membrane damage was assessed by quantifying the release of the cytoplasmic enzyme lactate dehydrogenase (LDH) from cells after insult (Kozeniewski and Callewaert, 1983). An LDH-release cytotoxicity kit II (Abcam) was used according to the manufacturer's protocol to measure the amount of LDH released into culture medium.

Statistical Analysis

Statistical analysis was performed by analysis of variance and Bonferroni post-test. $P < 0.05$ was considered statistically significant.

CHAPTER 3
RESULTS

Overexpression of SQSTM1

Expression of SQSTM1 and GFP in ARPE-19 cells was achieved using transfection techniques. Immunoblot analysis displayed increase of protein expression that appeared to reach a plateau at 1.5 µg of plasmid DNA (Fig. 3-1). Similarly, increasing transfecting DNA from 1.5 to 2.5 µg did not appear to lead to increased production of GFP. Expression levels of the respective proteins varied between three biological replicates (data not shown), displaying inconsistency in transfection efficiency. It is unknown whether the source of the inconsistency was the transfection reagent or a physiologic characteristic of the ARPE-19 cell line. Western blots were sensitive enough to detect basal levels of SQSTM1 (see no DNA control lane and pTR-smCBA-GFP transfection lanes).

Effect of Oxidative Stress on Viability and Proliferation Activity of ARPE-19 cells

To construct a dose response curve, untransfected ARPE-19 cells were exposed to increasing concentrations of hydrogen peroxide or 4-hydroxynonenal for 6 hours. The viability of ARPE-19 cells in response to increasing amounts of oxidative stress was measured using the MTT assay, which reflects the activity of NADH or NADPH redox enzymes inside cells. Samples of ARPE-19 cells without stressor were included as a negative control. Absorbance values of treated samples were compared to the untreated, untransfected control cells. ARPE-19 cells appeared to be resistant to treatment with lower levels of hydrogen peroxide. There is no significant difference in cells treated with 100 µM, 200 µM, or 400 µM H_2O_2 compared to the control (Fig. 3-2). Only 60% of the cells were still viable after 6 hours of incubation with 600 µM hydrogen

peroxide. Increasing hydrogen peroxide levels further led to an additional loss of cell viability by this measure. Treatment with 4-hydroxynonenal (4-HNE) led to a steeper threshold in viability. ARPE-19 cells were insensitive to 5 µM, 10 µM, and 20 µM, but MTT reduction was reduced by 75% at 40 µM and by 80 µM only 10% of the reducing activity was detected (Fig. 3-3). Fig. 3-2 and 3-3 display the mean of three independent experiments, each including samples performed in triplicate.

SQSTM1 Expression Does Not Protect ARPE-19 Cells From External Oxidative Stress

To determine if increased expression of SQSTM1 could protect ARPE-19 cell from oxidative stress, cells were transfected with 0.5 to 2.5 µg of pTR-SB-smCBA-SQSMT1 or pTR-SB-smCBA-GFP, and 48 hours later they were exposed to increasing levels of H_2O_2 ranging from 200 to 600 µM for 6 hours. Following this, cell viability was measured using the MTT assay as described (Fig. 3-4 - 3-6). No significant difference was seen in viability of cells expressing SQTSM1 in comparison to untransfected cells or cells expressing GFP. Similarly, to determine if increased expression of SQSTM1 could protect ARPE-19 cell from oxidative stress arising from 4-HNE, cells were transfected with 0.5 to 2.5 µg of pTR-SB-smCBA-SQSMT1 or pTR-SB-smCBA-GFP and 48 hours later they were exposed to 4-HNE levels ranging from 20-60 µM for 6 hours. Then cell viability was measured with the MTT assay (Fig. 3-7- 3-9). As for oxidative stress induced by hydrogen peroxide, increased expression of SQSTM1 did not lead to increased MTT reduction relative to untransfected cells or cells transfected with the GFP plasmid.

Overexpression of SQSTM1 Prevents Oxidative-Stress-Mediated Toxicity as Measured by Release of Lactate Dehydrogenase

Because the MTT assay depends on the activity of NADH or NADPH linked dehydrogenase enzymes, we also used an independent assessment of cytotoxicity of hydrogen peroxide and 4-HNE: release of lactate dehydrogenase (LDH). Lactate dehydrogenase is a cytoplasmic enzyme that interconverts lactate and pyruvate in the cells. Its release from the cytoplasm is widely used as a measure of cell integrity. Assessment of cell membrane integrity after 6 hours oxidative stress with H_2O_2 was achieved by measuring levels of lactate dehydrogenase released into the culture medium (Fig. 3-10). A significant difference was seen between GFP and SQSTM1 expressing cells treated with 800 μM hydrogen peroxide. This result suggests that overexpression of SQSTM1 may be able to prevent cytotoxicity related to oxidative stress in human RPE cells. Similarly, a significant increase in cytotoxicity was prevented in cells expressing SQSTM1 in comparison to the untransfected cells that were exposed to 4-hydroxynonenal for 6 hours (Fig. 3-11). However, there was no significant difference in cells that were expressing SQSTM1 in comparison to the GFP-expressing control cells.

HO-1 mRNA Levels are Increased Upon Exposure to Oxidative Stressors

Real-time polymerase chain reaction (RT-PCR) experiments were performed to determine if, when exposed to oxidative stress, induction of ARE enzymes in ARPE-19 cells is increased in cells overexpressing SQSTM1 (Fig. 3-12 - 3-15). ARPE-19 cells were transfected with 0.5 μg of pTR-SB-smCBA-SQSMT1 or pTR-SB-smCBA-GFP for 48 hours. At the end of this period, cells were exposed to either 800 μM hydrogen

peroxide or 40 μM 4-hydroxynonenal for 6 hours. Cells treated with the corresponding stressor and unstressed ARPE-19 cells and were included as controls. RT-PCR was used to determine mRNA levels of NQO1, HO-1, and GSTM1. GAPDH mRNA levels were analyzed and used an internal control. Results displayed represent either relative fold expression or expression after normalization to the GAPDH internal control. Results are the mean of three independent experiments, with samples read in duplicate for each experiment.

I hypothesized that increasing SQSTM1 expression would decrease cytosolic Keap1 availability, making cytosolic Nrf2 more available to be imported into the nucleus and upregulate ARE enzymes. HO-1 expression was upregulated in response to either 800 μM hydrogen peroxide or 40 μM 4-hydroxynonenal. Approximately a thirteen-fold and eighteen-fold increase in HO-1 response was observed in all samples after treatment with hydrogen peroxide and 4-hydroxynonenal, respectively, in comparison to untreated cells (Fig. 3-13, 3-15). Hydrogen peroxide instigated no increase in GSTM1 levels, but a two-fold increase in NQO1 levels was observed. 4-hydroxynonenal did not instigate an increase in NQO1 levels. However, a two-fold increase of GSTM1 mRNA levels was observed in control cells treated with the stressor and cells transfected with pTR-SB-smCBA-GFP. A slight decrease in GSTM1 expression was measured in cells transfected with pTR-SB-smCBA-SQSMT1. Because of the variability between replicates in this assay, the difference between cells transfected with pTR-SB-smCBA-SQSMT1 and pTR-SB-smCBA-GFP was not statistically significant.

Establishment of SQSTM1 Stable Cell Line

As an alternative to plasmid transfection, Lentiviral (LV)-mediated gene transfer was used to produce a cell line of human retinal pigment epithelial cells that

constitutively expresses *SQSTM1*. A cell line of ARPE-19 cells that constitutively expresses GFP was established concurrently as a control. LV-mediated gene transfer is a method that is more comparable to a gene therapy treatment in that a transgene coding for SQSTM1 will be delivered to cells and the gene of interest will be integrated into the host genome (Moldt, 2011). This method will abolish inconsistencies in results due to varying transfection efficiencies between biological replicates and cells transfected with different plasmids. Formation of this cell line will also allow us to examine the physiological effects of persistent expression of SQSTM1 in ARPE-19 cells. Selection of cells that produce the gene of interest was achieved by including a puromycin resistant gene downstream of the transgene. GFP production in the control cell line was effectively confirmed by fluorescence microscopy (Figure 3-16). Quantification of protein expression was accomplished by immunoblotting methods (Figure 3-17).

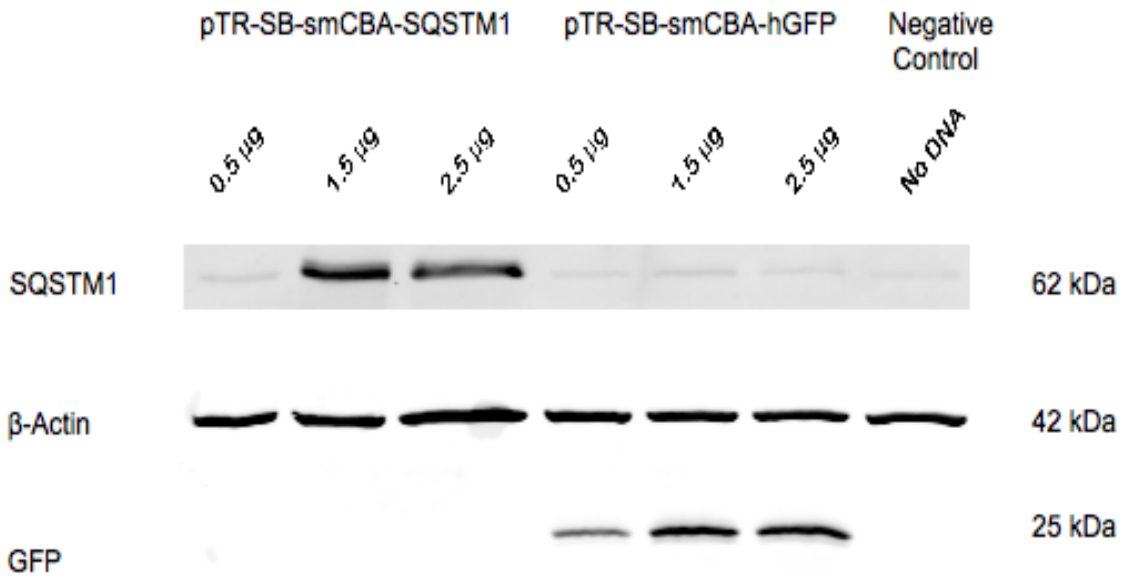

Figure 3-1. Immunoblot analysis of transfected ARPE-19 cells. Cells were transfected with increasing amounts of pTR-SB-smCBA-SQSTM1 or pTR-SB-smCBA-hGFP for 48 hours and lysate was run on a 10% Tris-HCl gel. Transfection with 0.5 µg plasmid DNA resulted in an increase in the quantity of the proteins of interest. Expression seemed to plateau when cells were transfected with 1.5 µg of DNA. Untransfected cells were included as a negative control. β-Actin was included as a loading control. Data presented is representative of one western blot. Three independent experiments were performed (data not shown).

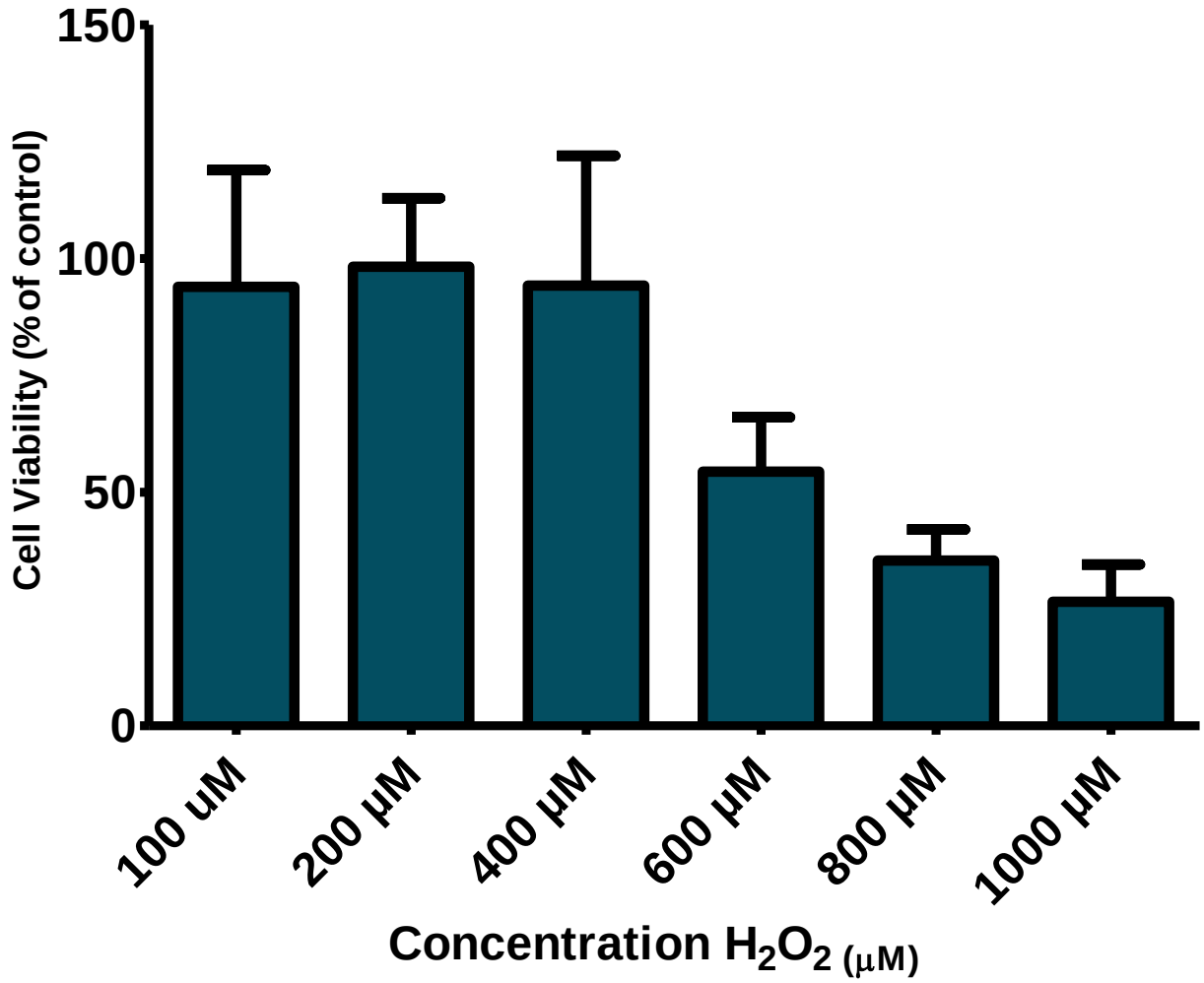

Figure 3-2. ARPE-19 response to increasing concentrations of hydrogen peroxide. Untransfected ARPE-19 cells were exposed to increasing concentrations of hydrogen peroxide for six hours in order to establish a dose response curve. Cell viability was assessed using an MTT Assay with samples analyzed in triplicate. Cells not exposed to oxidative stress were included as a negative control. Results are displayed as residual cellular viability relative to the negative control after induction of oxidative stress. Cells show no significant change in viability until they are exposed to 600 µM of hydrogen peroxide. Data are mean ± SD of three independent experiments.

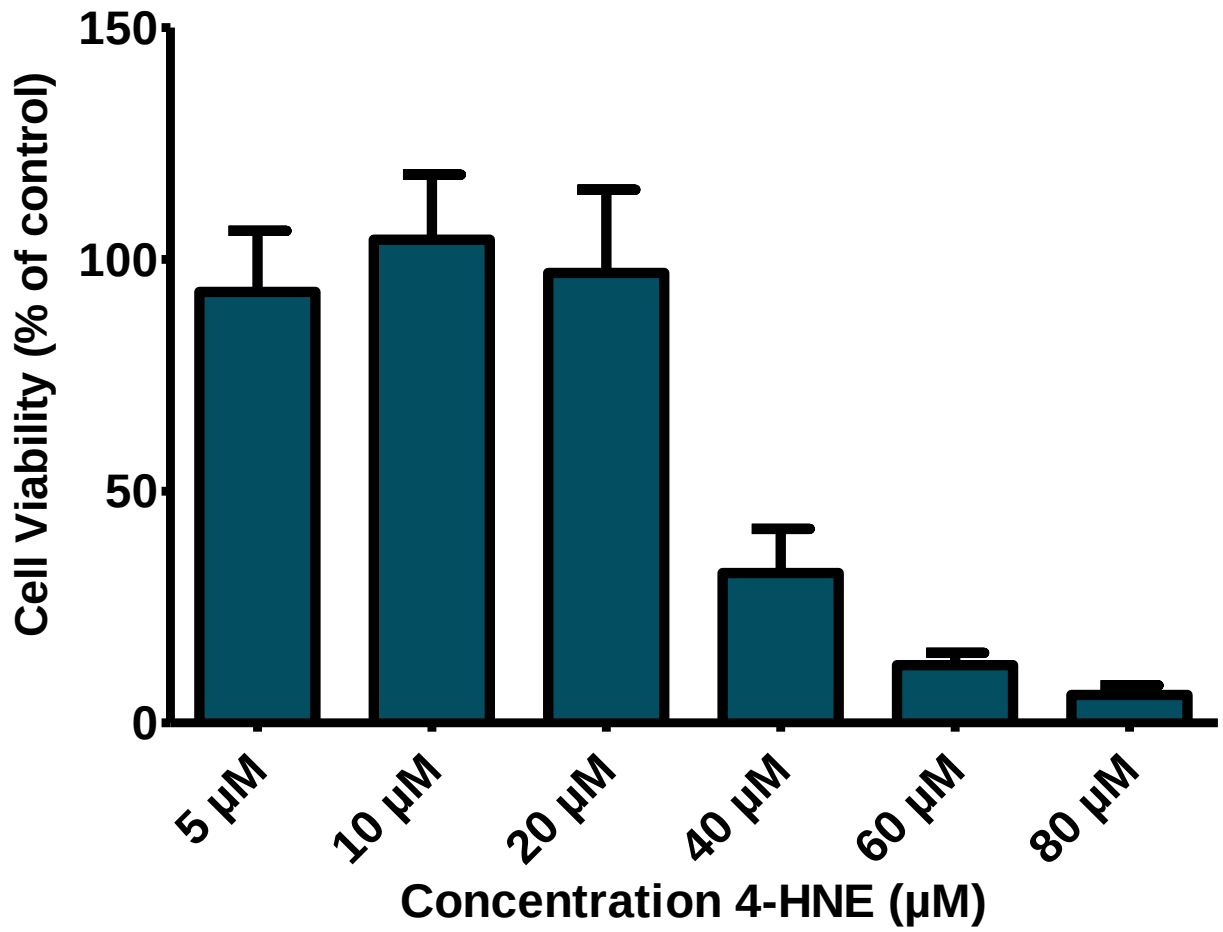

Figure 3-3. ARPE-19 response to increasing concentrations of 4-hydroxynonenal. Untransfected ARPE-10 cells were exposed to increasing concentrations of 4-hydroxynonenal for six hours in order to establish a dose response curve. Cell viability was assessed using an MTT Assay with samples analyzed in triplicate. Cells not exposed to oxidative stress were included as a negative control. Results are displayed as residual cellular viability relative to the negative control after induction of oxidative stress. Cells show no significant change in viability until they are exposed to 40 µM of 4-hydroxynonenal. Cell viability is severely affected at higher concentrations. Data are mean ± SD of three independent experiments.

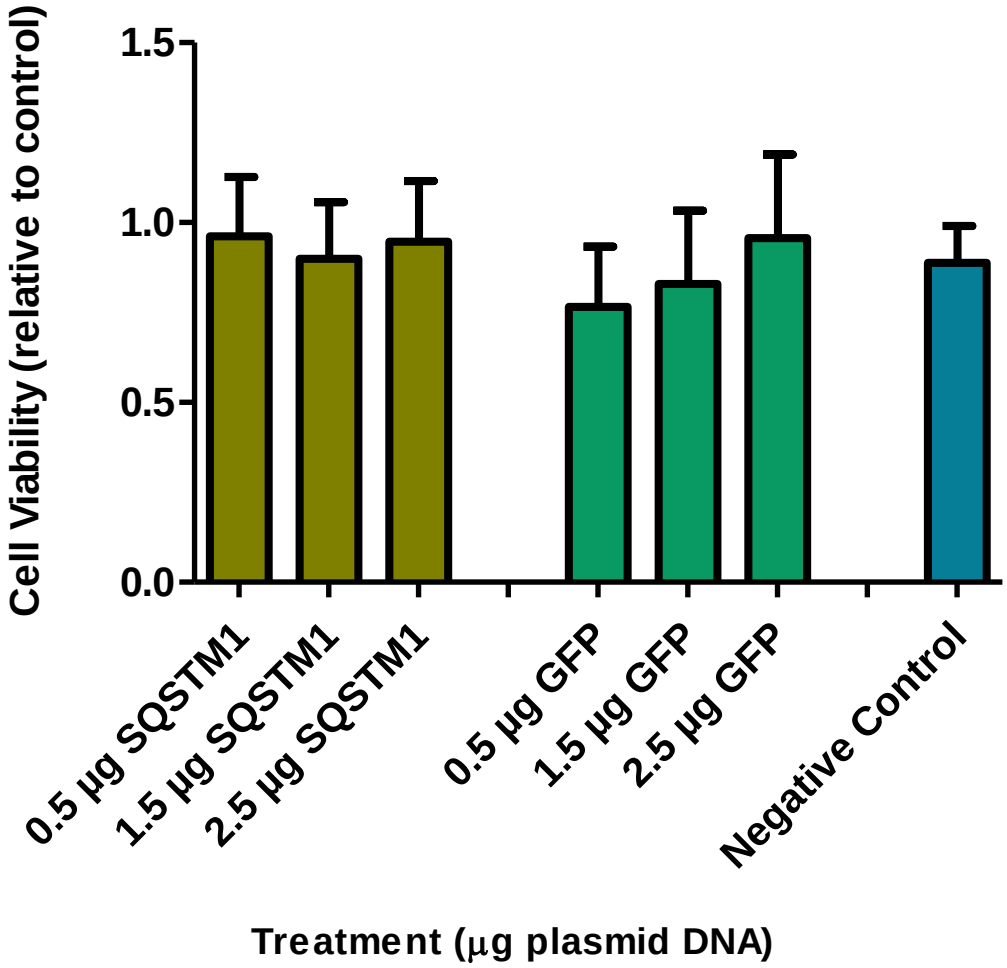

Figure 3-4. Transfected ARPE-19 response to 200 µM hydrogen peroxide. Cells were transfected with the indicated amount of plasmid DNA for 48 hours. Samples were then exposed to 200 µM hydrogen peroxide for six hours. Cellular viability was determined using an MTT assay with samples analyzed in triplicate. Untransfected ARPE-19 cells exposed to hydrogen peroxide are displayed on the graph as a negative control. A second negative control (not displayed) of ARPE-19 cells transfected with the indicated amount of plasmid DNA but not exposed to oxidative stress was included. Data is shown as residual cellular viability of each sample relative to the corresponding second negative control. Results are representative of the mean ± SD of three separate experiments.

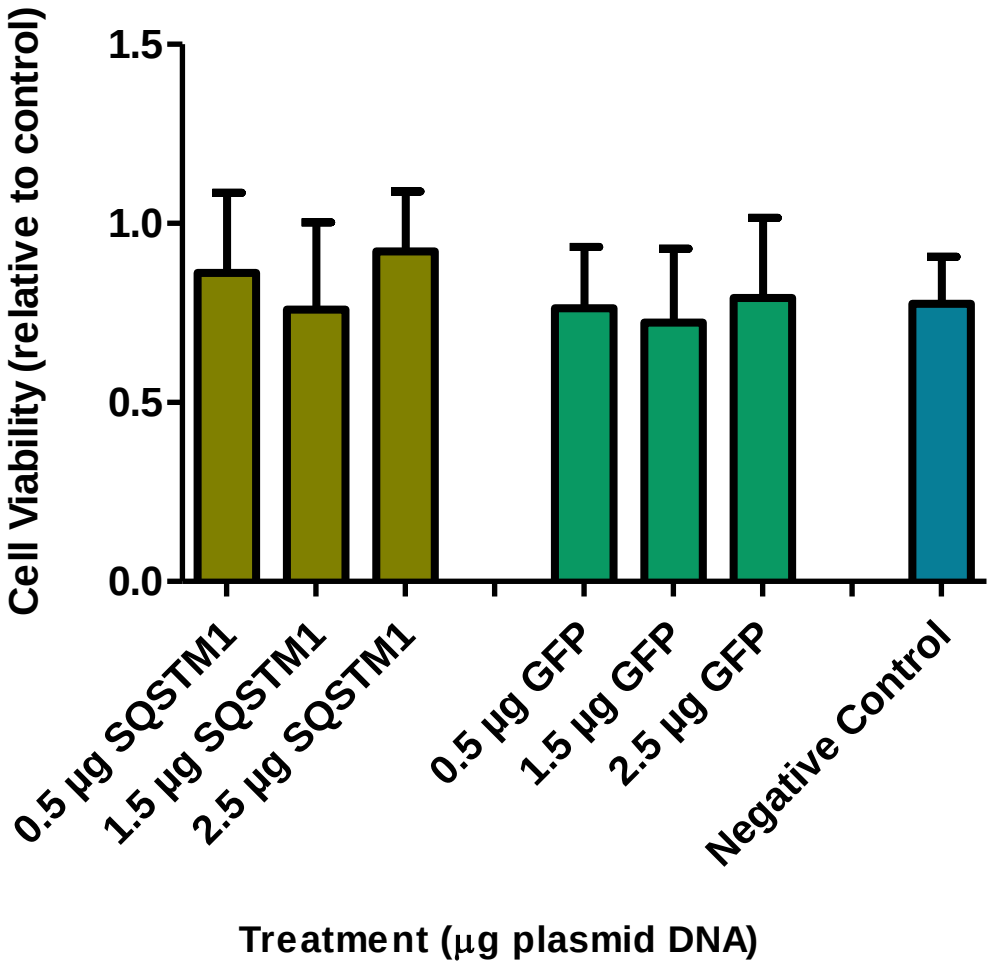

Figure 3-5. Transfected ARPE-19 response to 600 µM hydrogen peroxide. Cells were transfected with the indicated amount of plasmid DNA for 48 hours. Samples were then exposed to 600 µM hydrogen peroxide for six hours. Cellular viability was determined using an MTT assay with samples analyzed in triplicate. Untransfected ARPE-19 cells exposed to hydrogen peroxide are displayed on the graph as a negative control. A second negative control (not displayed) of ARPE-19 cells transfected with the indicated amount of plasmid DNA but not exposed to oxidative stress was included. Data is shown as residual cellular viability of each sample relative to the corresponding second negative control. Results are representative of the mean ± SD of three separate experiments.

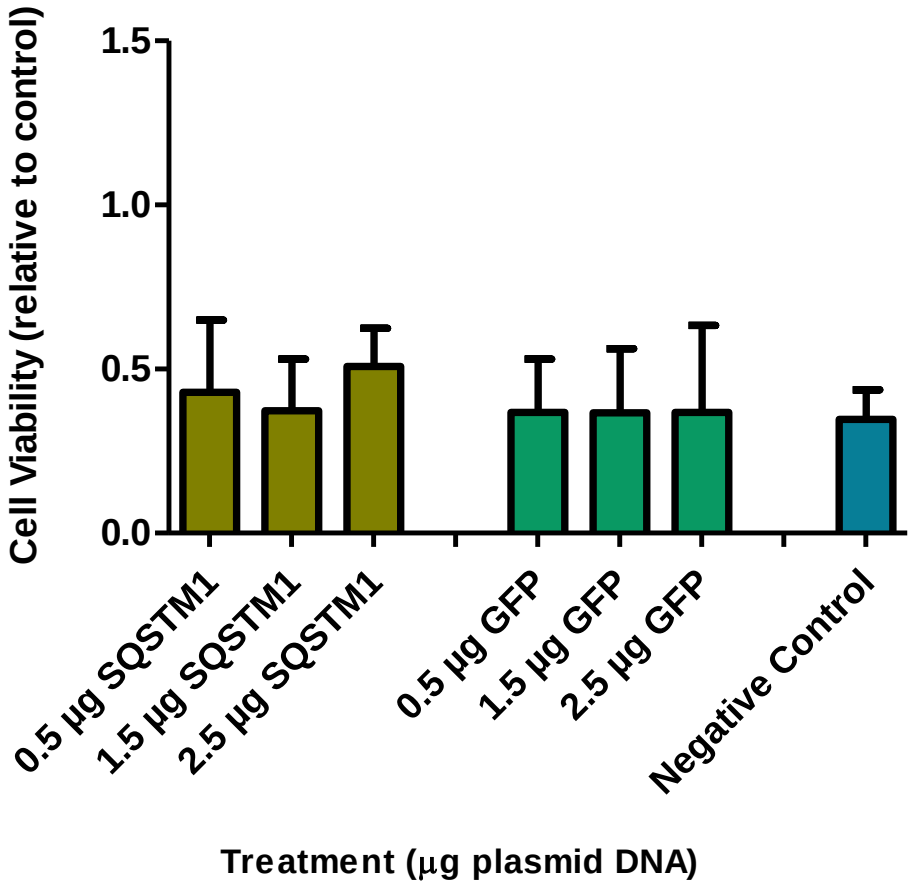

Figure 3-6. Transfected ARPE-19 response to 800 µM hydrogen peroxide. Cells were transfected with the indicated amount of plasmid DNA for 48 hours. Samples were then exposed to 800 µM hydrogen peroxide for six hours. Cellular viability was determined using an MTT assay with samples analyzed in triplicate. Untransfected ARPE-19 cells exposed to hydrogen peroxide are displayed on the graph as a negative control. A second negative control (not displayed) of ARPE-19 cells transfected with the indicated amount of plasmid DNA but not exposed to oxidative stress was included. Data is shown as residual cellular viability of each sample relative to the corresponding second negative control. Results are representative of the mean ± SD of three separate experiments.

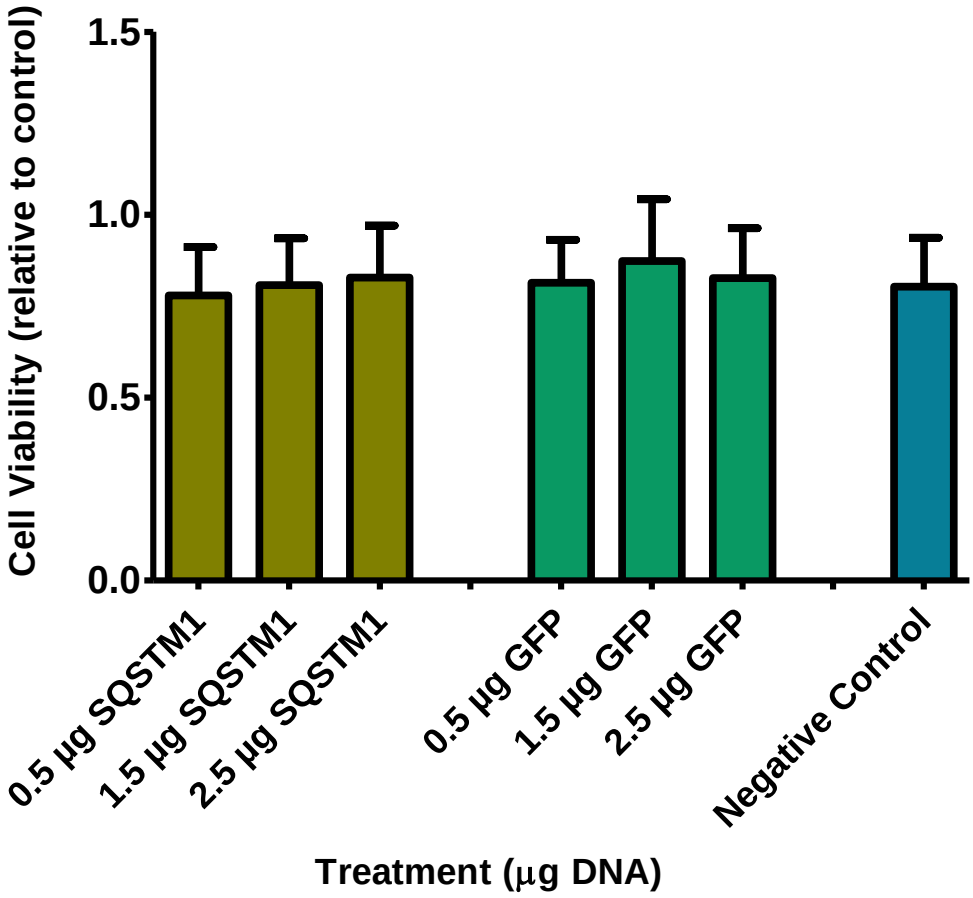

Figure 3-7. Effect of 20 µM 4-hydroxynonenal on ARPE-19 cell viability. Cells were transfected with the indicated amount of plasmid DNA for 48 hours. Samples were then exposed to 20 µM 4-hydroxynonenal for six hours. Cellular viability was determined using an MTT assay with samples analyzed in triplicate. A slight reduction in cell viability was detected amongst all samples. Untransfected ARPE-19 cells exposed to 4-hydroxynonenal are displayed on the graph as a negative control. A second negative control (not displayed) of ARPE-19 cells transfected with the indicated amount of plasmid DNA but not exposed to oxidative stress was included. Data is shown as residual cellular viability of each sample relative to the corresponding second negative control. Results are representative of the mean ± SD of three separate experiments.

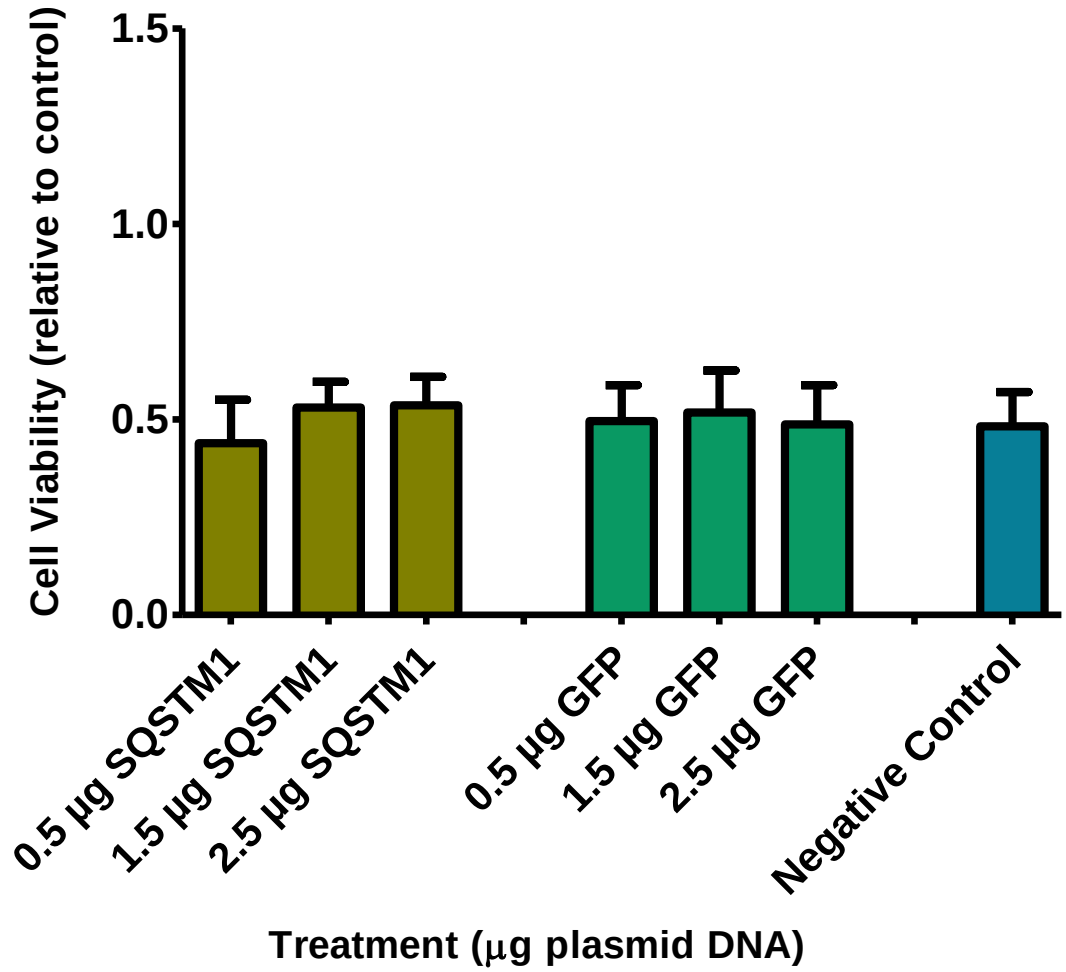

Figure 3-8. Effect of 40 µM 4-hydroxynonenal on ARPE-19 cell viability. Cells were transfected with the indicated amount of plasmid DNA for 48 hours. Samples were then exposed to 40 µM 4-hydroxynonenal for six hours. Cellular viability was determined using an MTT assay with samples analyzed in triplicate. Untransfected ARPE-19 cells exposed to 4-hydroxynonenal are displayed on the graph as a negative control. A second negative control (not displayed) of ARPE-19 cells transfected with the indicated amount of plasmid DNA but not exposed to oxidative stress was included. Data is shown as residual cellular viability of each sample relative to the corresponding second negative control. Results are representative of the mean ± SD of three separate experiments.

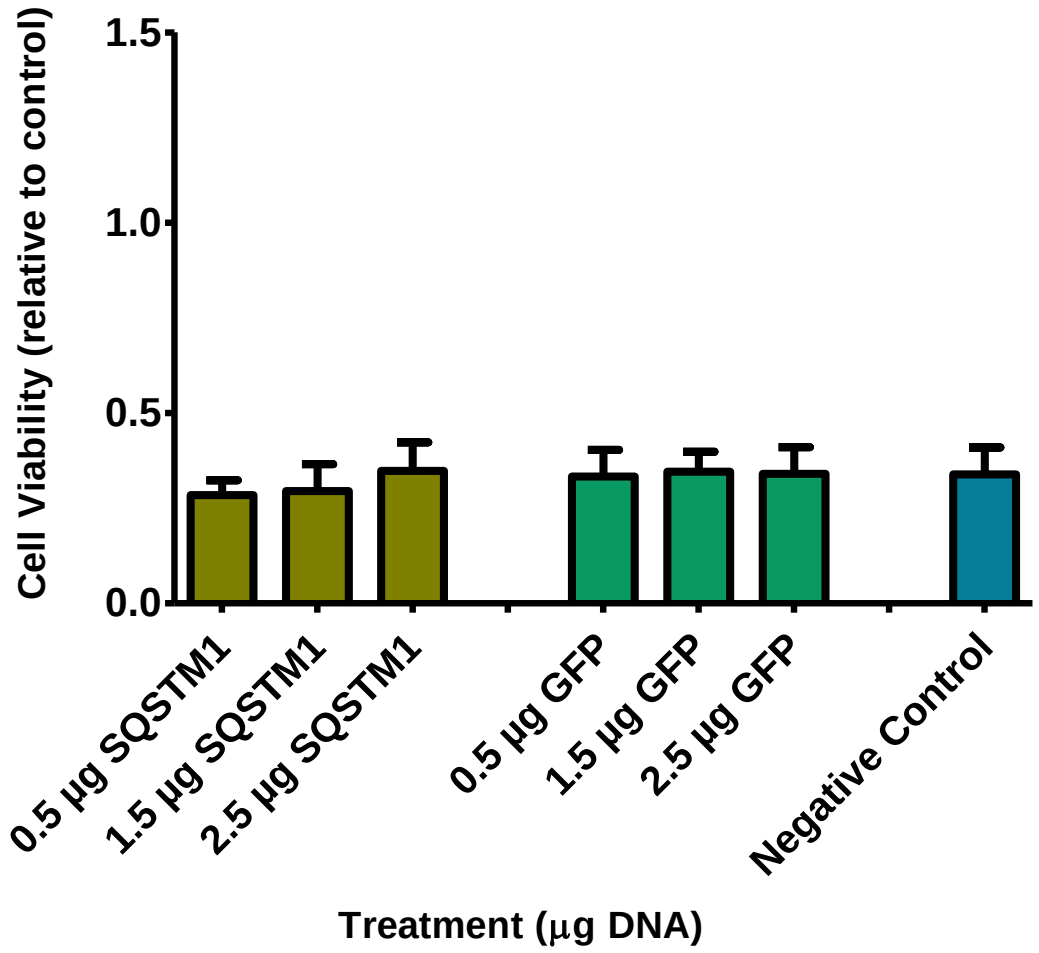

Figure 3-9. Effect of 60 µM 4-hydroxynonenal on ARPE-19 cell viability. Cells were transfected with the indicated amount of plasmid DNA for 48 hours. Samples were then exposed to 60 µM 4-hydroxynonenal for six hours. Cellular viability was determined using an MTT assay with samples analyzed in triplicate. Untransfected ARPE-19 cells exposed to 4-hydroxynonenal are displayed on the graph as a negative control. A second negative control (not displayed) of ARPE-19 cells transfected with the indicated amount of plasmid DNA but not exposed to oxidative stress was included. Data is shown as residual cellular viability of each sample relative to the corresponding second negative control. Results are representative of the mean ± SD of three separate experiments.

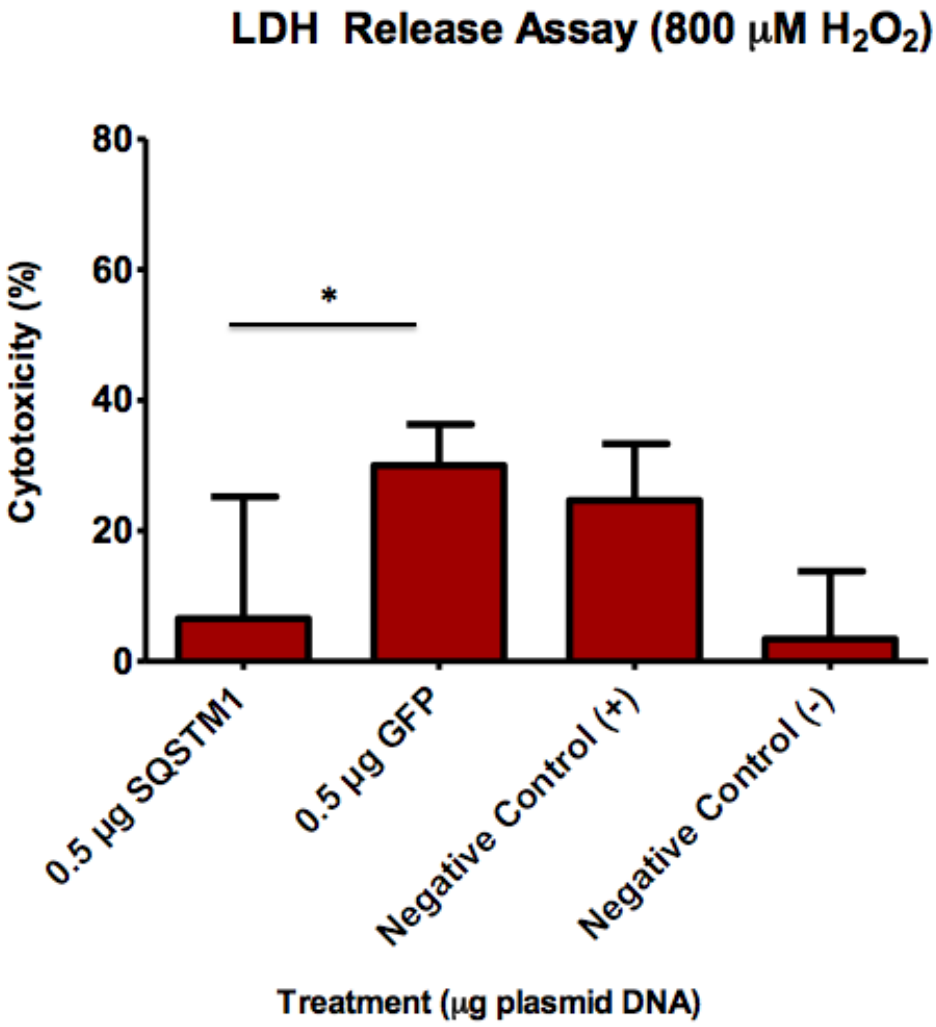

Figure 3-10. Lactate dehydrogenase (LDH) release as a measure of cytotoxicity in ARPE-19 cells treated with 800 μM hydrogen peroxide. ARPE-19 cells were transfected with 0.5 μg of pTR-SB-smCBA-SQSTM1 or pTR-SB-smCBA-GFP for 48 hours. Cells were then treated with 800 μM hydrogen peroxide for six hours. An LDH release assay was performed, with samples analyzed in duplicate, to quantify the amount of lactate dehydrogenase released into the medium of each sample after exposure to stress. A negative control of untransfected ARPE-19 cells treated with hydrogen peroxide is defined as NC (+). Likewise, untransfected cells that were not exposed to oxidative stress were included as another control and defined as NC (-). A reduction in cytotoxicity of cells expressing SQSTM1 was observed. Statistical significance was measured by analysis of variance, $P < 0.05$. Results shown represent the mean of three separate experiments ± SD.

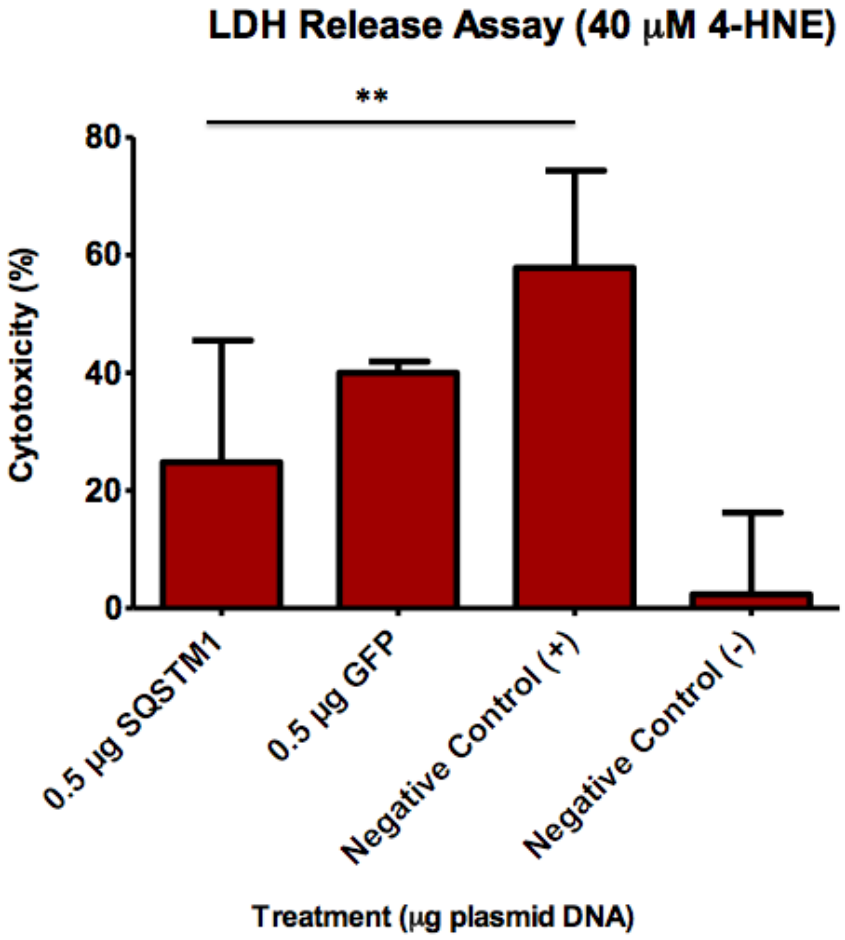

Figure 3-11. Lactate dehydrogenase (LDH) release as a measure of cytotoxicity in ARPE-19 cells treated with 40 μM 4-hydroxynonenal. ARPE-19 cells were transfected with 0.5 μg of pTR-SB-smCBA-SQSTM1 or pTR-SB-smCBA-GFP for 48 hours. Cells were then treated with 800 μM hydrogen peroxide for six hours. An LDH release assay was performed, with samples analyzed in duplicate, to quantify the amount of lactate dehydrogenase released into the medium of each sample after exposure to stress. A negative control of untransfected ARPE-19 cells treated with hydrogen peroxide is defined as NC (+). Likewise, untransfected cells that were not exposed to oxidative stress were included as another control and defined as NC (-). A reduction in cytotoxicity of cells expressing SQSTM1 compared to NC (+) was observed. Statistical significance was measured by analysis of variance, $P < 0.05$. Results shown represent the mean of three separate experiments ± SD.

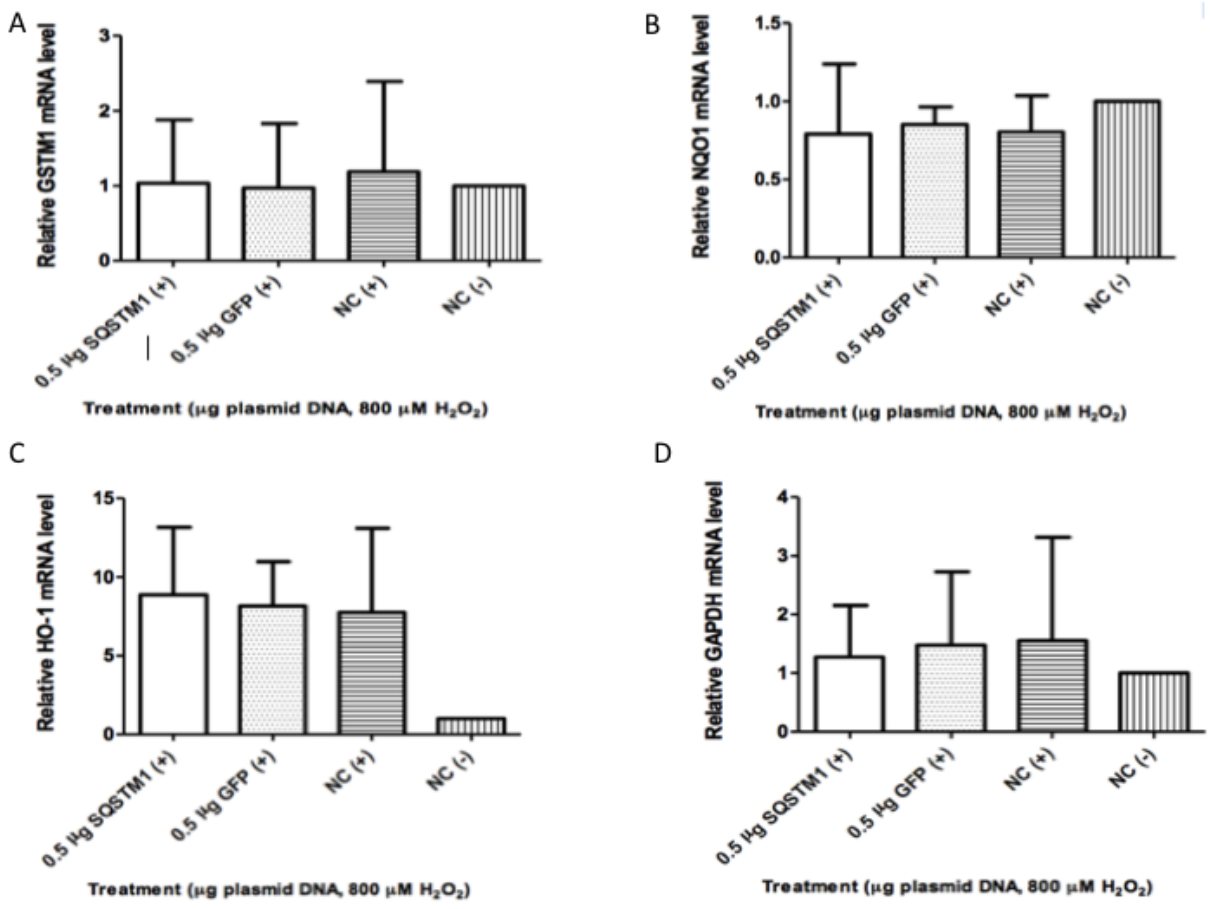

Figure 3-12. Relative Fold Expression of ARE antioxidant genes after insult with 800 µM hydrogen peroxide: A) GSTM1. B) NQO1. C) HO-1. D) GAPDH. ARPE-19 cells were transfected with 0.5 µg of pTR-SB-smCBA-SQSTM1 or pTR-SB-smCBA-GFP for 48 hours. Cells were then treated with H_2O_2 for six hours. RT-PCR was then performed to analyze change in mRNA levels of antioxidant genes. GAPDH levels were measured as an internal control. A negative control of untransfected ARPE-19 cells treated with hydrogen peroxide is defined as NC (+). Likewise, untransfected cells that were not exposed to oxidative stress were included as another control and defined as NC (-). Results are displayed as mRNA levels relative to NC (-). Data shown represent the mean of three separate experiments ± SD.

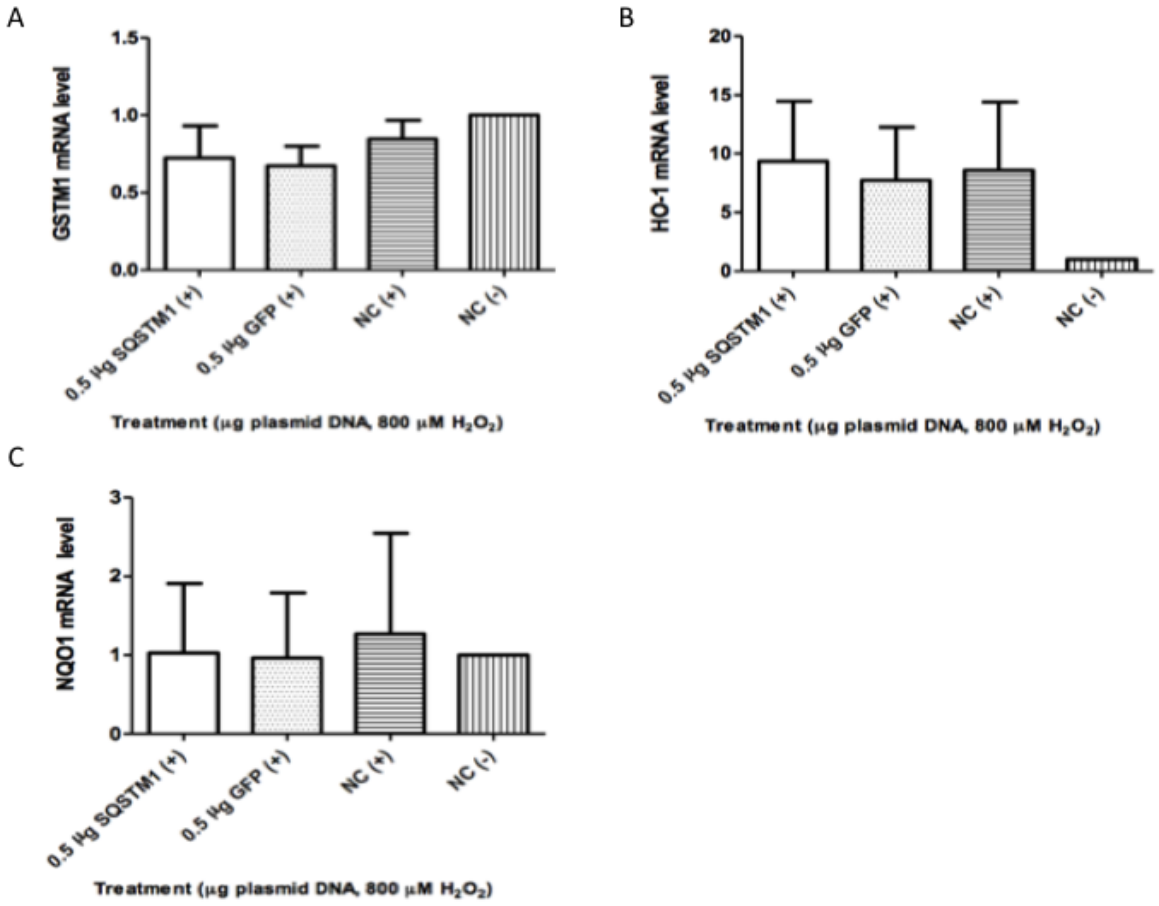

Figure 3-13. mRNA levels of ARE antioxidant genes after insult with 800 µM hydrogen peroxide. Expression of ARE antioxidant genes after insult with 800 µM hydrogen peroxide normalized to GAPDH mRNA levels. A) GSTM1. B) HO-1. C) NQO1. ARPE-19 cells were transfected with 0.5 µg of pTR-SB-smCBA-SQSTM1 or pTR-SB-smCBA-GFP for 48 hours. Cells were then treated with H_2O_2 for six hours. RT-PCR was then performed to analyze change in mRNA levels of antioxidant genes. A negative control of untransfected ARPE-19 cells treated with hydrogen peroxide is defined as NC (+). Likewise, untransfected cells that were not exposed to oxidative stress were included as another control and defined as NC (-). Results are displayed as mRNA levels relative to NC (-). Data shown represent the mean of three separate experiments ± SD.

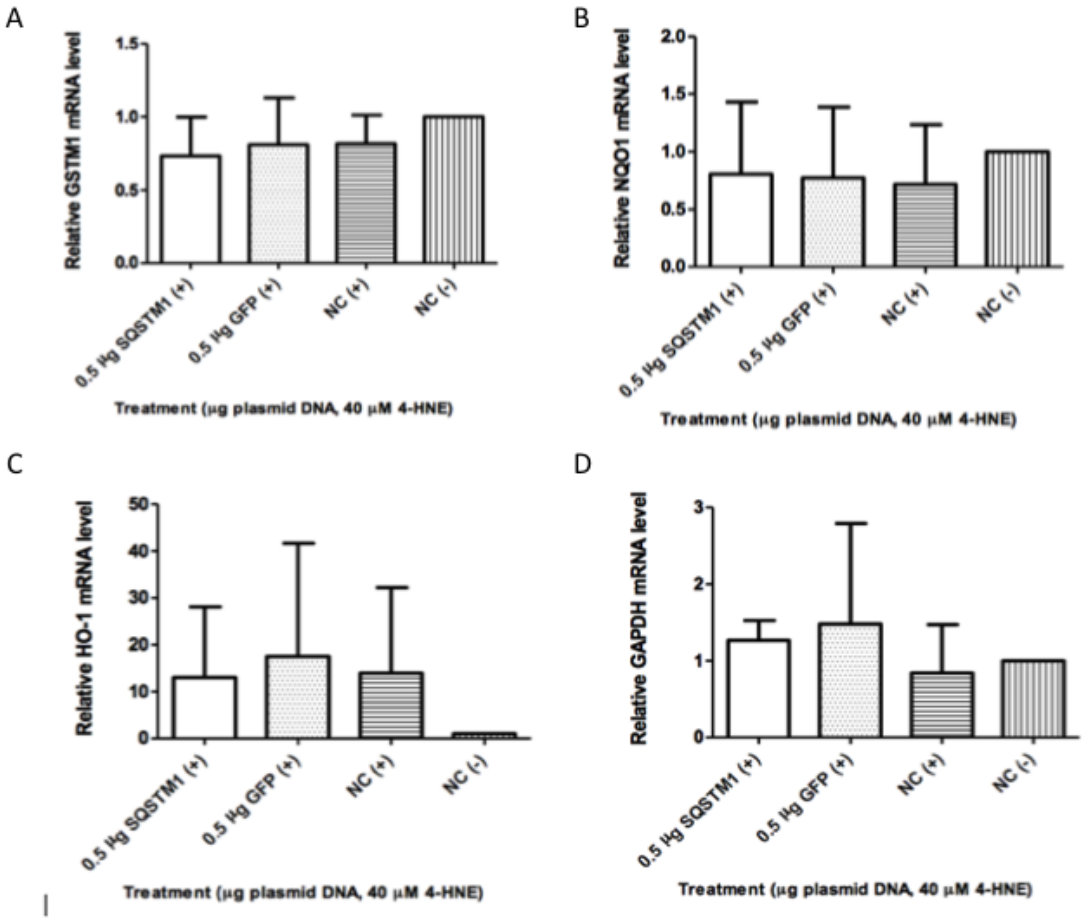

Figure 3-14. Relative Fold Expression of ARE antioxidant genes after insult with 40 µM 4-hydroxynonenal. A) GSTM1. B) NQO1. C) HO-1. D) GAPDH. ARPE-19 cells were transfected with 0.5 µg of pTR-SB-smCBA-SQSTM1 or pTR-SB-smCBA-GFP for 48 hours. Cells were then treated with 4-HNE for six hours. RT-PCR was then performed to analyze change in mRNA levels of antioxidant genes. GAPDH levels were measured as an internal control. A negative control of untransfected ARPE-19 cells treated with hydrogen peroxide is defined as NC (+). Likewise, untransfected cells that were not exposed to oxidative stress were included as another control and defined as NC (-). Results are displayed as mRNA levels relative to NC (-). Data shown represent the mean of three separate experiments ± SD.

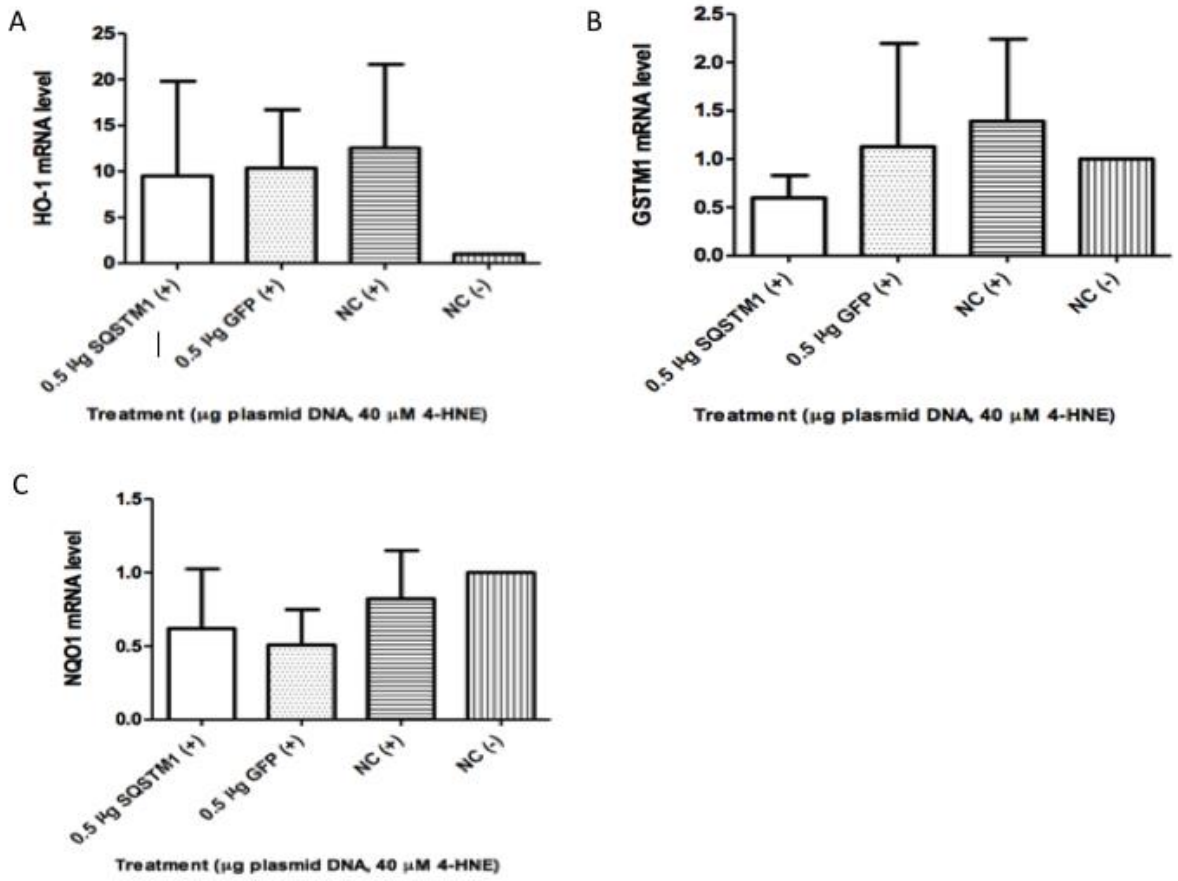

Figure 3-15. mRNA levels of ARE antioxidant genes after insult with 40 µM 4-hydroxynonenal. Expression of ARE antioxidant genes after insult with 40 µM 4-hydroxynonenal normalized to GAPDH mRNA levels. A) HO-1. B) GSTM1. C) NQO1. ARPE-19 cells were transfected with 0.5 µg of pTR-SB-smCBA-SQSTM1 or pTR-SB-smCBA-GFP for 48 hours. Cells were then treated with 4-HNE for six hours. RT-PCR was then performed to analyze change in mRNA levels of antioxidant genes. A negative control of untransfected ARPE-19 cells treated with hydrogen peroxide is defined as NC (+). Likewise, untransfected cells that were not exposed to oxidative stress were included as another control and defined as NC (-). Results are displayed as mRNA levels relative to NC (-). Data shown represent the mean of three separate experiments ± SD.

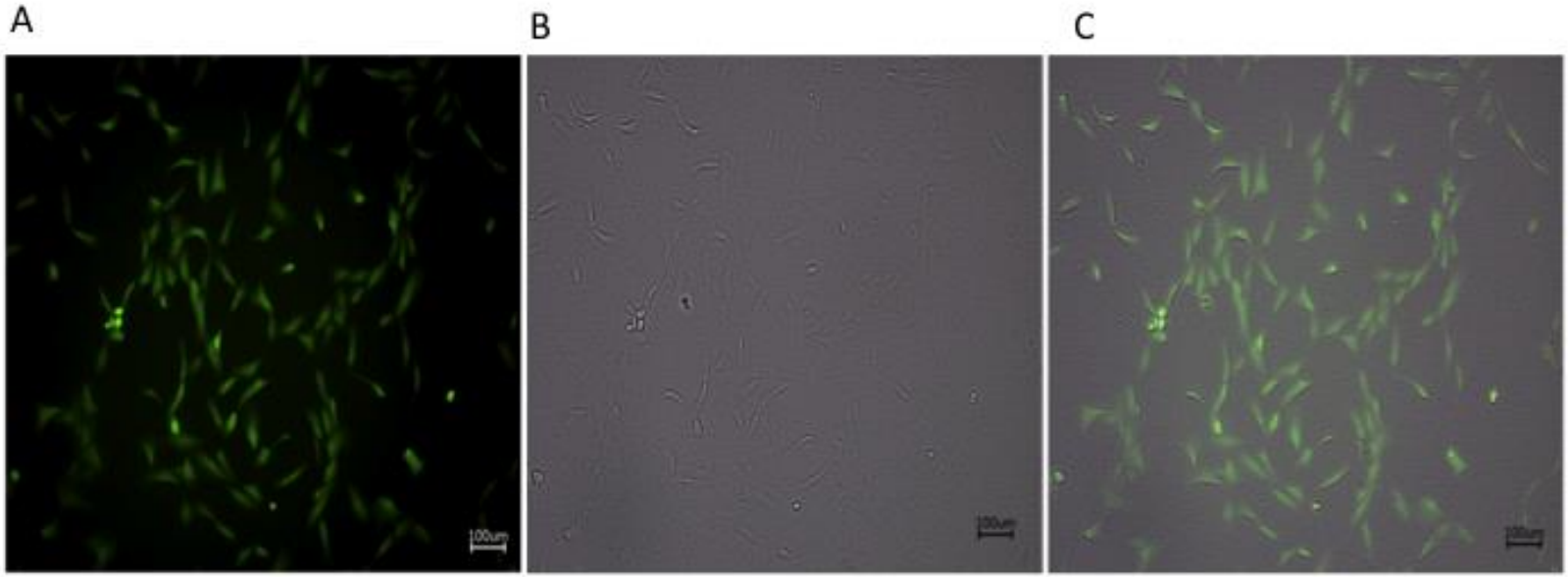

Figure 3-16. Verification of GFP Expression in GFP stable cell line. Fluorescence microscopy was used to assess if the cells were expressing the transgene of interest. A) GFP stable ARPE-19 cells displayed expression of the GFP transgene in ARPE-19 cells that persisted after selection. B) SQSTM1 stable ARPE-19 cells lacked expression of GFP. C) An overlay of the images in (A) and (B).

Figure 3-17. Immunoblot analysis depicting SQSTM1 or GFP levels of stable cell lines. Cell lysates were extracted and run on a 10% Tris-HCl gel. Expression of SQSTM1 or GFP can be seen in the sample extract. Densitometry was performed using ImageJ. β-actin was included as a loading control. This experiment was performed once, with all samples displayed representative of one western blot.

CHAPTER 4
DISCUSSION AND CONCLUSIONS

The results of these experiments confirm that we were able to successfully overexpress SQSTM1 in ARPE-19 cells without seeing a drastic change in cell viability in comparison to wild-type ARPE-19 cells. However, the ability of SQSTM1 to activate the Nrf2/ARE cascade and aid in protection against oxidative stress is not clear.

It is evident that mitochondrial respiratory activity is sensitive to oxidative stress. It is important to note that hydrogen peroxide and 4-hydroxynonenal differed in their ability to instigate dysfunction of cellular capabilities. ARPE-19 cells were able to maintain cell viability at higher concentrations of hydrogen peroxide than 4-hydroxynonenal. In accordance with other studies, both hydrogen peroxide and 4-hydroxynonenal induced HO-1 expression in RPE cells (Pilat, 2013; Huang, 2012). Unfortunately, SQSTM1 overexpression did not instigate a more robust HO-1 response than in the other controls. Future studies may include delivery of SQSTM1 to the RPE in a mouse model of dry AMD. This would allow us to determine if SQSTM1 overexpression would protect mitochondrial function in the context of the disease state.

Previously published studies have established that transfection of SQSTM1 cDNA protects primary cortical neuron cells from oxidative stress via the Nrf2/KEAP1/ARE pathway. Upon overexpression of *SQSTM1* cDNA, NQO1 protein expression was increased 2.6-fold, as verified by western blot (Liu, 2007). Although our results confirm a slight increase in *NQO1* transcript levels (2.0-fold) after exposure to hydrogen peroxide, the increase was the same in ARPE-19 cells overexpressing SQSTM1 as it was in both transfected and untransfected controls. In fact, untransfected ARPE-19 cells exposed to hydrogen peroxide displayed greater *NQO1* expression than

in GFP- or SQSTM1- expressing cells. This may indicate that transient transfection methods instigate the induction of ARE enzymes and might serve as a source of cellular stress. The conflict between our results and those of the Liu group may be due to cell type specificity or to the relative quantity of SQSTM1 overexpression. Overexpression of SQSTM1 may modulate the KEAP1/Nrf2/ARE pathway in the same manner but to a different extent in primary cortical culture.

Necrosis and apoptosis are two distinct mechanisms of cell death. Necrosis is characterized by injury to cytoplasmic organelles, cell swelling, membrane lysis, and release of cytoplasmic contents. Apoptosis is characterized by membrane blebbing, shrinkage of the cell, chromatin condensation, and cross-linking of membrane proteins (Bonfoco, 1995). These processes differ in many ways, but importantly here, in the release of cellular content into the neighboring environment. The results of the LDH assays suggest that SQSTM1-expressing cells released significantly less lactate dehydrogenase than in untreated ARPE-19 cells that were exposed to stress. In order to make further conclusions about overall cellular health from these results, it is necessary to determine if the apoptotic pathway was initiated in SQSTM1 expressing cells. It is possible that apoptosis but not primary or secondary necrosis was initiated in SQSTM1-expressing cells, preventing the release of LDH into the medium but not offering protection to the mitochondria in the MTT assays. It is also possible that SQSTM1 overexpression mediated protection from cell death, but not mitochondrial dysfunction, by a pathway other than the ARE.

The additional roles that SQSTM1 plays in the cell must be taken into consideration when determining if overexpression of this protein will offer attenuation of

oxidative stress-induced damage. Further studies may include identifying the location of overexpressed SQSTM1 using immunocytochemistry. Importantly, it has been demonstrated that SQSTM1 is subject to nucleocytoplasmic shuffling in order to participate in multiple pathways (Pankiv, 2010). It is also known that accumulation of SQSTM1 can result in its inclusion in p62 or PML bodies in the nucleus (Pankiv, 2010).

If overexpressed SQSTM1 is confined within these bodies or homodimerizes in the nucleus, sufficient sequestration of KEAP1 may not be occurring. In this case, the Nrf2/KEAP1/ARE pathway may not be responsible for the protection displayed in Figs. 3-6 and 3-7. This proposal, of course, is dependent on the rate of SQSTM1 nuclear import and export, whether nuclear export of SQSTM1 is a saturable process, and the percentage of overexpressed or endogenous SQSTM1 that is appropriated into protein aggregates. A greater understanding of these events could shed light on the results that we report.

Lastly, the positive feedback loop created by Nrf2 and SQSTM1 should not be ignored. In correlation with its role in Nrf2 induction, SQSTM1 levels increase after oxidative stress (Ishii, 1997). This interaction must be considered. If overexpressing SQSTM1 by transfecting with 0.5 μg of plasmid DNA leads to toxic levels of either Nrf2 or SQSTM1, then our methods may be injurious to cellular function. Importantly, this may not interfere with plasmid membrane tenacity resulting from cell death, explaining the conflicting results in the MTT and LDH release assays. However, there may be an optimal degree of SQSTM1 overexpression for our desired purposes that can lead to nontoxic levels of nuclear Nrf2 to induce ARE expression.

In order to further investigate the role of SQSTM1 in protection from oxidative stress without the interfering effects of a transfection reagent, ARPE-19 cell lines that constitutively express SQSTM1 or GFP were established. Further studies using these cell lines will need to be performed in order to assess the feasibility of a gene therapy treatment geared toward overexpressing SQSTM1 in the RPE. This cell line will be able to demonstrate the effects of viral vector-based delivery of SQSTM1 to RPE cells.

In conclusion, it is still possible that overexpression of SQSTM1 may mediate protection of retinal pigment epithelial cells from oxidative stress, although its ability to protect certain features of the cell may differ. Altering the Nrf2/ARE pathway by increasing SQSTM1 availability will need to be investigated *in vivo* in order to fully assess the potential of this alteration as a gene therapy treatment for dry-AMD patients.

REFERENCES

Arshavsky, V.Y., and Burns, M.E. (2012). Photoreceptor signaling: supporting vision across a wide range of light intensities. J Biol Chem *287*, 1620-1626.

Barnett, B.P., and Handa, J.T. (2013). Retinal Microenvironment Imbalance in Dry Age-Related Macular Degeneration: A Mini-Review. Gerontology.

Bird, A.C. (2010). Therapeutic targets in age-related macular disease. J Clin Invest *120*, 3033-3041.

Bjørkøy, G., Lamark, T., Brech, A., Outzen, H., Perander, M., Overvatn, A., Stenmark, H., and Johansen, T. (2005). p62/SQSTM1 forms protein aggregates degraded by autophagy and has a protective effect on huntingtin-induced cell death. J Cell Biol *171*, 603-614.

Blasiak, J., Glowacki, S., Kauppinen, A., and Kaarniranta, K. (2013). Mitochondrial and nuclear DNA damage and repair in age-related macular degeneration. Int J Mol Sci *14*, 2996-3010.

Bonfoco, E., Krainc, D., Ankarcrona, M., Nicotera, P., and Lipton, S.A. (1995). Apoptosis and necrosis: two distinct events induced, respectively, by mild and intense insults with N-methyl-D-aspartate or nitric oxide/superoxide in cortical cell cultures. Proc Natl Acad Sci U S A *92*, 7162-7166.

Campa, C., Costagliola, C., Incorvaia, C., Sheridan, C., Semeraro, F., De Nadai, K., Sebastiani, A., and Parmeggiani, F. (2010). Inflammatory mediators and angiogenic factors in choroidal neovascularization: pathogenetic interactions and therapeutic implications. Mediators Inflamm *2010*.

Cheung, L.K., and Eaton, A. (2013). Age-Related Macular Degeneration. Pharmacotherapy.

Duboff, B., Feany, M., and Götz, J. (2013). Why size matters - balancing mitochondrial dynamics in Alzheimer's disease. Trends Neurosci.

Dunn, K.C., Aotaki-Keen, A.E., Putkey, F.R., and Hjelmeland, L.M. (1996). ARPE-19, a human retinal pigment epithelial cell line with differentiated properties. Exp Eye Res *62*, 155-169.

Fan, W., Tang, Z., Chen, D., Moughon, D., Ding, X., Chen, S., Zhu, M., and Zhong, Q. (2010). Keap1 facilitates p62-mediated ubiquitin aggregate clearance via autophagy. Autophagy *6*, 614-621.

Garg, S., Oran, A.E., Hon, H., and Jacob, J. (2004). The hybrid cytomegalovirus enhancer/chicken beta-actin promoter along with woodchuck hepatitis virus posttranscriptional regulatory element enhances the protective efficacy of DNA vaccines. J Immunol *173*, 550-558.

Geetha, T., and Wooten, M.W. (2002). Structure and functional properties of the ubiquitin binding protein p62. FEBS Lett *512*, 19-24.

Gutierrez, P.L. (2000). The metabolism of quinone-containing alkylating agents: free radical production and measurement. Front Biosci *5*, D629-638.

Ha, K.N., Chen, Y., Cai, J., and Sternberg, P. (2006). Increased glutathione synthesis through an ARE-Nrf2-dependent pathway by zinc in the RPE: implication for protection against oxidative stress. Invest Ophthalmol Vis Sci *47*, 2709-2715.

Halliwell, B. (2006). Reactive species and antioxidants. Redox biology is a fundamental theme of aerobic life. Plant Physiol *141*, 312-322.

He, Y., Ge, J., Burke, J.M., Myers, R.L., Dong, Z.Z., and Tombran-Tink, J. (2010). Mitochondria impairment correlates with increased sensitivity of aging RPE cells to oxidative stress. J Ocul Biol Dis Infor *3*, 92-108.

Huang, Y., Li, W., and Kong, A.N. (2012). Anti-oxidative stress regulator NF-E2-related factor 2 mediates the adaptive induction of antioxidant and detoxifying enzymes by lipid peroxidation metabolite 4-hydroxynonenal. Cell Biosci *2*, 40.

Ishii, T., Yanagawa, T., Yuki, K., Kawane, T., Yoshida, H., and Bannai, S. (1997). Low micromolar levels of hydrogen peroxide and proteasome inhibitors induce the 60-kDa A170 stress protein in murine peritoneal macrophages. Biochem Biophys Res Commun *232*, 33-37.

Jain, A., Lamark, T., Sjøttem, E., Larsen, K.B., Awuh, J.A., Øvervatn, A., McMahon, M., Hayes, J.D., and Johansen, T. (2010). p62/SQSTM1 is a target gene for transcription factor NRF2 and creates a positive feedback loop by inducing antioxidant response element-driven gene transcription. J Biol Chem *285*, 22576-22591.

Jarrett, S.G., Lewin, A.S., and Boulton, M.E. (2010). The importance of mitochondria in age-related and inherited eye disorders. Ophthalmic Res *44*, 179-190.

Kaneda, M. (2013). Signal processing in the Mammalian retina. J Nippon Med Sch *80*, 16-24.

Khandhadia, S., Cherry, J., and Lotery, A.J. (2012). Age-related macular degeneration. Adv Exp Med Biol *724*, 15-36.

Klein, R., Chou, C.F., Klein, B.E., Zhang, X., Meuer, S.M., and Saaddine, J.B. (2011). Prevalence of age-related macular degeneration in the US population. Arch Ophthalmol *129*, 75-80.

Koopman, W.J., Verkaart, S., Visch, H.J., van Emst-de Vries, S., Nijtmans, L.G., Smeitink, J.A., and Willems, P.H. (2007). Human NADH:ubiquinone oxidoreductase deficiency: radical changes in mitochondrial morphology? Am J Physiol Cell Physiol *293*, C22-29.

Korzeniewski, C., and Callewaert, D.M. (1983). An enzyme-release assay for natural cytotoxicity. J Immunol Methods *64*, 313-320.

Krohne, T.U., Stratmann, N.K., Kopitz, J., and Holz, F.G. (2010). Effects of lipid peroxidation products on lipofuscinogenesis and autophagy in human retinal pigment epithelial cells. Exp Eye Res *90*, 465-471.

Kubli, D.A., and Gustafsson, Å. (2012). Mitochondria and mitophagy: the yin and yang of cell death control. Circ Res *111*, 1208-1221.

Kwong, J.Q., Henning, M.S., Starkov, A.A., and Manfredi, G. (2007). The mitochondrial respiratory chain is a modulator of apoptosis. J Cell Biol *179*, 1163-1177.

Laemmli, U.K. (1970). Cleavage of structural proteins during the assembly of the head of bacteriophage T4. Nature *227*, 680-685.

Liu, Y., Kern, J.T., Walker, J.R., Johnson, J.A., Schultz, P.G., and Luesch, H. (2007). A genomic screen for activators of the antioxidant response element. Proc Natl Acad Sci U S A *104*, 5205-5210.

Moldt, B., Miskey, C., Staunstrup, N.H., Gogol-Döring, A., Bak, R.O., Sharma, N., Mátés, L., Izsvák, Z., Chen, W., Ivics, Z.*, et al.* (2011). Comparative genomic integration profiling of Sleeping Beauty transposons mobilized with high efficacy from integrase-defective lentiviral vectors in primary human cells. Mol Ther *19*, 1499-1510.

Narendra, D., Kane, L.A., Hauser, D.N., Fearnley, I.M., and Youle, R.J. (2010). p62/SQSTM1 is required for Parkin-induced mitochondrial clustering but not mitophagy; VDAC1 is dispensable for both. Autophagy *6*, 1090-1106.

Nezis, I.P., and Stenmark, H. (2012). p62 at the interface of autophagy, oxidative stress signaling, and cancer. Antioxid Redox Signal *17*, 786-793.

Nguyen, T., Nioi, P., and Pickett, C.B. (2009). The Nrf2-antioxidant response element signaling pathway and its activation by oxidative stress. J Biol Chem *284*, 13291-13295.

Olszewska, A., and Szewczyk, A. (2013). Mitochondria as a pharmacological target: magnum overview. IUBMB Life *65*, 273-281.

Pankiv, S., Lamark, T., Bruun, J.A., Øvervatn, A., Bjørkøy, G., and Johansen, T. (2010). Nucleocytoplasmic shuttling of p62/SQSTM1 and its role in recruitment of nuclear polyubiquitinated proteins to promyelocytic leukemia bodies. J Biol Chem *285*, 5941-5953.

Pilat, A., Herrnreiter, A.M., Skumatz, C.M., Sarna, T., and Burke, J.M. (2013). Oxidative stress increases HO-1 expression in ARPE-19 cells, but melanosomes suppress the increase when light is the stressor. Invest Ophthalmol Vis Sci *54*, 47-56.

Plafker, S.M., O'Mealey, G.B., and Szweda, L.I. (2012). Mechanisms for countering oxidative stress and damage in retinal pigment epithelium. Int Rev Cell Mol Biol *298*, 135-177.

Reuland, D.J., Khademi, S., Castle, C.J., Irwin, D.C., McCord, J.M., Miller, B.F., and Hamilton, K.L. (2013). Upregulation of phase II enzymes through phytochemical activation of Nrf2 protects cardiomyocytes against oxidant stress. Free Radic Biol Med *56*, 102-111.

Rodríguez-Muela, N., Koga, H., García-Ledo, L., de la Villa, P., de la Rosa, E.J., Cuervo, A.M., and Boya, P. (2013). Balance between autophagic pathways preserves retinal homeostasis. Aging Cell.

Santos, J.M., Mohammad, G., Zhong, Q., and Kowluru, R.A. (2011). Diabetic retinopathy, superoxide damage and antioxidants. Curr Pharm Biotechnol *12*, 352-361.

Schreiber, A., and Peter, M. (2013). Substrate recognition in selective autophagy and the ubiquitin-proteasome system. Biochim Biophys Acta.

Strauss, O. (2005). The retinal pigment epithelium in visual function. Physiol Rev *85*, 845-881.

Tew, K.D. (2011). NrF2/Keap1 as gatekeepers of redox homeostasis – do they prevent or cause cancer? Pigment Cell Melanoma Res *24*, 1078-1079.

Tezel, G. (2011). The immune response in glaucoma: a perspective on the roles of oxidative stress. Exp Eye Res *93*, 178-186.

Voleti, V.B., and Hubschman, J.P. (2013). Age-related eye disease. Maturitas.

Wenzel, P., Schuhmacher, S., Kienhöfer, J., Müller, J., Hortmann, M., Oelze, M., Schulz, E., Treiber, N., Kawamoto, T., Scharffetter-Kochanek, K.*, et al.* (2008). Manganese superoxide dismutase and aldehyde dehydrogenase deficiency increase mitochondrial oxidative stress and aggravate age-dependent vascular dysfunction. Cardiovasc Res *80*, 280-289.

Yau, K.W., and Hardie, R.C. (2009). Phototransduction motifs and variations. Cell *139*, 246-264.

BIOGRAPHICAL SKETCH

Danielle Lorna Liverpool was born in Danbury, CT to Joseph and Kathleen Liverpool. She was raised in Brandon, FL by a loving family that included her parents and her older brother, Stephen Liverpool. Although she was diagnosed with terminal cancer at the age of 13, she continues to relentlessly pursue life with strong faith and a joyful attitude. As a grandchild of four immigrants from the small island of St. Vincent, having the opportunity to pursue higher education has made a tremendous impact in her life.

She is the second member of her family to attend the University of Florida. Her research endeavors and thought-provoking classes inspired her to pursue a career in the biotechnology industry. In May 2011, she obtained her Bachelor of Science degree in biology with a specialization in biotechnology. After completing the requirements for her master of science degree, she will continue to pursue a career in biotechnology.